

# Pattern Formation in Random Networks Using Graphons

Jason Bramburger<sup>1</sup> and Matt Holzer<sup>1,2</sup>

<sup>1</sup>Department of Mathematical Sciences, George Mason University, Fairfax, VA, USA

<sup>2</sup>Center for Mathematics and Artificial Intelligence (CMAI), George Mason University, Fairfax, VA, USA

## Abstract

We study Turing bifurcations on one-dimensional random ring networks where the probability of a connection between two nodes depends on the distance between the two nodes. Our approach uses the theory of graphons to approximate the graph Laplacian in the limit as the number of nodes tends to infinity by a nonlocal operator – the graphon Laplacian. For the ring networks considered here, we employ center manifold theory to characterize Turing bifurcations in the continuum limit in a manner similar to the classical partial differential equation case and classify these bifurcations as sub/super/trans-critical. We derive estimates that relate the eigenvalues and eigenvectors of the finite graph Laplacian to those of the graphon Laplacian. We are then able to show that, for a sufficiently large realization of the network, with high probability the bifurcations that occur in the finite graph are well approximated by those in the graphon limit. The number of nodes required depends on the spectral gap between the critical eigenvalue and the remaining ones, with the smaller this gap the more nodes that are required to guarantee that the graphon and graph bifurcations are similar. We demonstrate that if this condition is not satisfied then the bifurcations that occur in the finite network can differ significantly from those in the graphon limit.

**Keywords:** Turing bifurcation, random graph, graphon, center manifold

**MSC numbers:** 37L10, 35R02, 92C15, 60B20

## 1 Introduction

Diffusive instabilities occur when a stable homogeneous state is destabilized in the presence of diffusion. These instabilities form a common pathway to the spontaneous self-organization of patterned states. Alan Turing discovered these bifurcations in work aimed at explaining the emergence of patterns during morphogenesis [41], and today these instabilities are often referred to as Turing bifurcations. Turing bifurcations have been shown to be a dominant mechanism for pattern formation in a number of applications including biology [15, 25, 38], chemistry [9, 39], neuroscience [8, 14] and ecology [23, 32] and similar mechanisms are known to drive pattern formation in fluids [12, 36] and bacterial aggregation [22].

In this work we will study Turing bifurcations occurring in complex networks described by random graphs with a particular focus on ring networks where the likelihood of connection between nodes is dependent on

the distance between nodes. An obvious challenge in the study of bifurcations on random graphs is deriving results that hold independently of the realization of the network with high probability. To accomplish this we will appeal to the theory of graph limits utilizing graphons; see [27]. For a fixed random graph model, in the limit as the number of nodes goes to infinity, graphons approximate the adjacency matrix (or in our case the graph Laplacian) of the finite graph by a non-local operator. The integral kernel of this operator is called the graphon, which derives from graph function. For the ring networks studied here, the graphon exactly describes the probability of connections between nodes as a function of the distance between them. The question then becomes, essentially, how well we can predict the character of Turing bifurcations in the random graph based only upon some mean-field approximation of the average likelihood of a connection between nodes based upon their distance.

A number of previous studies have focused on Turing bifurcations in complex networks. For cellular networks, Turing instabilities were studied in [38] with a particular focus on several classes of regular networks. In [35], instability criterion are derived in analogy with the partial differential equation (PDE) theory where the onset of instability can be expressed as a function of the Laplacian eigenvalues. In [43] it is demonstrated that for scale-free networks these bifurcations are typically transcritical and lead to the appearance of highly localized patterns dominated by a small number of differentiated nodes. Snaking properties of these localized patterns were subsequently analyzed in [29]. Further studies of this phenomena include [19, 33, 34], to only name a few. We also mention recent work on Turing patterns in zebrafish resulting from nonlocal, distance-dependent interactions between cells [24, 42]. In a somewhat different direction, the study of localized pattern formation in the discrete spatial setting has been studied previously on infinite chains [5, 6], square lattices [7], and rings [40]. We also mention in passing the prevalence of non-local, distance dependent coupling in neural field models; see for example [1, 8, 18].

Our approach using graphons in this manuscript is motivated by recent work where graphons are used to approximate the interaction graph in a coupled oscillator problem and to derive bifurcations to synchrony in this mean-field limit, as was done in [10, 11]. Other utilizations of graphons in the study of dynamical systems on random graphs include [21, 30, 31] for nonlinear heat equations and [26] for power networks.

The theory of graph limits via graphons is the primary analytical tool that we use in this work (in addition to center manifold theory). Graphons were introduced in [2, 3] and the simplest way to visualize one is as a pixel plot of the adjacency matrix for a graph. The idea is that, for some classes of random graphs, the sequence of realizations of the graph adjacency matrix will converge to a non-local operator as the number of vertices tends to infinity with many features of the graphs being preserved in the limit. For our purposes here, we will be interested in how well the eigenvalues and eigenvectors of the random graph Laplacian will be approximated by the eigenvalues and eigenfunctions of the graphon Laplacian. Informally speaking, in scenarios where there this approximation is sufficiently accurate we will be able to show that the bifurcations occurring on the graph closely mimic the bifurcations occurring for the graphon. More precisely, we will use spectral convergence results presented in [20, 27], modified to the case of the graph Laplacian using the approach of [37], followed by an application of a version of the Davis-Kahan Theorem [13, 44] to control the difference between the graph Laplacian eigenvectors and the graphon eigenfunctions. We refer the interested reader to [2, 3, 16, 20, 27, 28] and references therein for more complete introductions to the theory of graph limits and graphons.

Let us now set the stage for the problem considering herein. Consider a network described as a connected, un-weighted, un-directed graph  $G = (V, E)$  with  $|V| = N$ . In this paper, we will study the following system

of ordinary differential equations, known as the Swift-Hohenberg equation, and given by

$$\frac{du}{dt} = -(\mathbf{L} - \kappa\mathbf{I})^2 u + \varepsilon u + ru \circ u - bu \circ u \circ u. \quad (1.1)$$

Here  $\kappa$ ,  $r$  and  $b > 0$  are parameters and  $u \circ u$  is the Hadamard, or component-wise, product of vectors. The matrix  $\mathbf{L}$  is the graph Laplacian associated to the graph  $G$  which describes interactions between connected elements on the graph. Throughout this work we will exclusively work with the combinatorial Laplacian defined by  $\mathbf{L} = \mathbf{A} - \mathbf{D}$ , where  $\mathbf{A}$  is the *adjacency matrix* and  $\mathbf{D}$  is the diagonal matrix composed of row sums of  $\mathbf{A}$ , termed the *degree matrix*. The Swift-Hohenberg equation is a model equation for systems undergoing a Turing bifurcation [12], thus making it an optimal phenomenological model for our study of such bifurcations in the discrete spatial setting of graph networks. We point out that the nonlinearity in (1.1) can be viewed as a Taylor expansion of a more general nonlinearity. For the purposes of our analysis we only require terms up to cubic order and so we simply omit any higher order terms to simplify the presentation.

The criterion for diffusive instability in (1.1) is analogous to that of the PDE case, as described in [35]. The graph Laplacian  $\mathbf{L}$  has eigenvalues  $\lambda_k \leq 0$  and normalized eigenvectors  $v_k$ , and so letting  $\mathbf{M} = -(\mathbf{L} - \kappa\mathbf{I})^2$  means that the  $v_k$  remain eigenvectors of  $\mathbf{M}$ , now with eigenvalues

$$\ell_k = -\lambda_k^2 + 2\kappa\lambda_k - \kappa^2. \quad (1.2)$$

Note that if  $\lambda_k = \kappa$  for some  $k$  then the homogeneous trivial state,  $u = 0$ , in (1.1) will be unstable for any  $\varepsilon > 0$ . Since (1.1) is a system of nonlinear ODEs we may apply center manifold reduction techniques to characterize the bifurcation that occurs. When  $\mathbf{L}$  is the graph Laplacian for an arbitrary complex network it is typically the case that the bifurcation occurring at  $\varepsilon = 0$  has co-dimension one and, owing to the preservation of the zero solution, the reduced equation on the center manifold then takes the form

$$\frac{dw_1}{dt} = \varepsilon w_1 + a_2 w_1^2 + a_3 w_1^3 + \mathcal{O}(w_1^4, w_1^2 \varepsilon), \quad (1.3)$$

for some constants  $a_2$  and  $a_3$ . The bifurcation can then be classified as transcritical if  $a_2 \neq 0$  and as a sub (super)-critical pitchfork if  $a_2 = 0$  and  $a_3 > 0$  ( $a_3 < 0$ ). If  $v_1$  is the marginally stable eigenvector then the coefficient  $a_2 = rv_1^T(v_1 \circ v_1)$  measures interactions of the bifurcating mode with itself under the quadratic coupling term.

We emphasize that for complex networks we expect  $a_2 \neq 0$  and therefore the resulting bifurcation is generically transcritical. This is exactly what the analysis for scale-free networks has revealed [43]. However, an important distinction exists for ring networks studied herein. We will show that for sufficiently large realizations of these networks the isolated eigenvalues possess eigenvectors that are approximated by discrete Fourier basis vectors. Such Fourier basis vectors have the property that they do not exhibit any self-interaction under the quadratic coupling in (1.1) – hence  $a_2 = 0$  for the mean-field limit. This will be one of the main analytical results of this paper. Informally, if our random graph Laplacian has a sufficiently isolated eigenvalue and the number of nodes is sufficiently large, then the corresponding eigenvector will be well approximated by a discrete Fourier basis vector and therefore  $a_2 \approx 0$ . From (1.3), the accompanying Turing bifurcation on the random graph is transcritical with a saddle-node bifurcation nearby, coming from perturbing the mean-field pitchfork bifurcation. Theorem 4.1 below provides a precise statement of this result.

The remainder of the paper is organized as follows. In Section 2 we review the notion of a graphon and derive our main approximation results that relate the eigenvalues and eigenvectors of the random graph Laplacian to the spectrum and eigenfunctions of the graphon Laplacian operator. In Section 3, we apply infinite dimensional center manifold theory to classify bifurcations for the non-local graphon Laplacian operator. In Section 4, we apply the results from Section 2 to derive analogous bifurcation results on for the random graph Laplacian for realizations of the random network with a sufficiently large number of nodes. In Section 5, we study some examples numerically both to lend credence to our main results and to demonstrate what happens when the bifurcating eigenvalue is not isolated or an insufficiently large realization of the network is taken. We conclude with a discussion of our results and areas for future exploration in Section 6.

## 2 Graphons as Graph Limits

As stated in the introduction, our goal is to investigate bifurcations from the trivial state of the spatially discrete Swift–Hohenberg equation (1.1). In particular, we are interested in large graphs,  $|V| = N \gg 1$ , and therefore we turn to understanding their formal limiting objects as  $N \rightarrow \infty$ . In the following subsection we will review the relevant definitions on graph limits, termed graphons, and then in the subsections that follow we present a number of auxiliary results that describe the limiting behaviour of the spectrum of (1.1) linearized about  $u = 0$  in the large  $N$  limit. We take the perspective that we start with the limiting graphon and show how it can be used to define both deterministic and random graphs, which are treated separately in Section 2.2 and Section 2.3, respectively. Our review of graphons is in no way meant to be complete and therefore we direct the interested reader to [2, 3, 16, 20, 27, 28] for a more thorough introduction and treatment of them.

### 2.1 Preliminaries

At the most general level a *graphon* is a symmetric Lebesgue-measurable function  $W : [0, 1]^2 \rightarrow [0, 1]$  which, for simplicity, we will assume is continuous almost-everywhere in  $[0, 1]^2$ . A simple consequence of the fact that  $0 \leq W \leq 1$  is that  $W$  has finite  $L^p := L^p([0, 1]^2)$  norm,

$$\|W\|_p := \left( \int_{[0,1]^2} |W(x, y)|^p dx dy \right)^{\frac{1}{p}} \leq 1, \quad (2.1)$$

for all  $p \in [1, \infty)$  and similarly  $\|W\|_\infty \leq 1$ . The term graphon derives from “graph function” and they have the property that they approximate the pixel plot of an adjacency matrix in the limit as the number of vertices tends to infinity. Hence, this formalism can be used to obtain a non-local version of the graph Laplacian, denoted  $\mathcal{L}_W$  and termed a *graphon Laplacian* throughout, acting on functions  $f : [0, 1] \rightarrow \mathbb{C}$  by

$$\mathcal{L}_W f(x) = \int_0^1 W(x, y) (f(y) - f(x)) dy, \quad \forall x \in [0, 1]. \quad (2.2)$$

In the limit as the number of vertices of the graph goes to infinity, formally (1.1) takes the form

$$\frac{du}{dt} = -(\mathcal{L}_W - \kappa)^2 u + \varepsilon u + ru^2 - bu^3. \quad (2.3)$$

With the definition of a graphon Laplacian comes the notion of the degree of a vertex  $x \in [0, 1]$ , given by

$$\text{Deg}(W)(x) := \int_0^1 W(x, y) dy, \quad (2.4)$$

which can be interpreted as the formal limit of the degree matrix associated to a graph Laplacian.

Such graphon Laplacians can be seen as operators acting between  $L^p$  spaces, and so we will consider the norm for linear operators mapping  $L^p \rightarrow L^q$ , given by

$$\|\mathcal{L}_W\|_{p \rightarrow q} := \sup_{\|f\|_p=1} \|\mathcal{L}_W f\|_q. \quad (2.5)$$

In what follows we will primarily be concerned with the case  $p = q = 2$  since  $L^2$  is a Hilbert space, thus allowing one to project onto eigenspaces. Moreover, notice that the symmetry  $W(x, y) = W(y, x)$  of the graphon  $W$  implies that  $\mathcal{L}_W : L^2 \rightarrow L^2$  is self-adjoint. One may use the uniform boundedness of  $\|W\|_p$  to verify that  $\|\mathcal{L}_W\|_{p \rightarrow q} < \infty$  for all  $p, q \in [1, \infty]$ , thus making the graphon Laplacian operator continuous from any  $L^p$  space into another.

Following [10], we will use a graphon  $W$  to construct finite graphs with  $N$  vertices in two different ways. In both cases the unit interval is discretized with  $x_j = \frac{j}{N}$  with  $j = 0, \dots, N - 1$ . We will refrain from including the dependence on  $N$  for all finite graphs generated by the graphon to simplify the notation. A *deterministic weighted graph* with adjacency matrix  $A_d = [A_{i,j}]_{1 \leq i, j \leq N}$  is obtained by setting

$$A_{ij} = \begin{cases} W\left(\frac{i}{N}, \frac{j}{N}\right) & i \neq j \\ 0 & i = j \end{cases}. \quad (2.6)$$

The restriction that  $A_{i,i} = 0$  means that the associated graph does not contain any loops (edges that originate and terminate at the same vertex). This restriction is merely for the ease of presentation since it can be observed in (2.2) that the diagonal terms have no effect in the graphon Laplacian. Similarly, these loops have no effect when moving to a finite graph and considering the associated (combinatorial) graph Laplacian

$$L_d := A_d - \text{Deg}(A_d), \quad (2.7)$$

where  $\text{Deg}(A_d)$  is the diagonal degree matrix whose entries are the sums of the rows of  $A_d$ .

Alternatively, we may obtain a *random graph* by considering a binary adjacency matrix  $A_r = [\xi_{i,j}]_{1 \leq i, j \leq N}$  whose elements  $\xi_{i,j} \in \{0, 1\}$  are random variables with probability distribution

$$\mathbb{P}(\xi_{ij} = 1) = 1 - \mathbb{P}(\xi_{ij} = 0) = W\left(\frac{i}{N}, \frac{j}{N}\right) \quad (2.8)$$

for  $i \neq j$  and  $\xi_{i,i} = 0$  for all  $1 \leq i \leq N$ . Setting the diagonal elements of  $A_r$  to zero again has the effect that we do not consider loops in the resulting graph. As above, this adjacency matrix leads to a graph Laplacian operator associated to a graph with  $N$  vertices, denoted

$$L_r := A_r - \text{Deg}(A_r), \quad (2.9)$$

where  $\text{Deg}(A_r)$  is again the diagonal degree matrix whose entries are the sums of the rows of  $A_r$ . It should be noted that we may further consider the points  $x_i \in [0, 1]$  to be drawn randomly [2, 31] and obtain the

deterministic and random graphs as above, but we refrain from doing this for the ease of presentation. The reader should keep in mind that all of the results presented in the following subsections will carry over to the randomly chosen  $x_i$ , should an application necessitate it.

Let us consider some motivating examples.

**Example 2.1.** (i) For some  $p \in [0, 1]$  we can define an **Erdős–Réyni** graph using the graphon  $W(x, y) = p$  for all  $x, y \in [0, 1]$ . In this case the associated deterministic weighted graph on  $N$  vertices has every vertex connected to every other vertex with an edge weight of  $p$ , while the random graph assigns an edge of weight 1 between any two vertices with probability  $p$ .

(ii) For parameters  $p, q, \alpha \in [0, 1]$  the graphon

$$W(x, y) = \begin{cases} p & \text{if } |x - y| \bmod 1 \leq \alpha \\ q & \text{if } |x - y| \bmod 1 > \alpha \end{cases} \quad (2.10)$$

is used to generate a **small-world**, or **Watts–Strogatz**, graph. The resulting deterministic graph is a ring such that each vertex is connected to all others, but vertices within a distance of  $\alpha$  (with respect to the ring distance) have edge weight  $p$ , otherwise the edge weight is  $q$ . In the random graph case the probability of having a connection between two vertices is  $p$  if they are within a distance of  $\alpha$ , otherwise the probability is  $q$ .

(iii) For some  $p \in (0, 1]$  and  $\alpha \in (0, 1)$  a **bipartite** graph can be formed through the graphon

$$W(x, y) = \begin{cases} p & \text{if } \min\{x, y\} \leq \alpha, \max\{x, y\} > \alpha \\ 0 & \text{otherwise} \end{cases} \quad (2.11)$$

The resulting deterministic graph has an edge with weight  $p$  between each  $x_i \in [0, \alpha]$  and  $x_j \in (\alpha, 1]$ , while the random graph assigns such edges with probability  $p$ . No edges are present between two  $x_i$  that both belong to either  $[0, \alpha]$  or  $(\alpha, 1]$ .

In this work we will focus exclusively on “ring” networks. These networks are characterized by graphons taking the form  $W(|x - y|)$ , where the argument  $|x - y|$  is to be considered modulo 1. Such graphons have the property that

$$\text{Deg}(x) = \int_0^1 \tilde{W}(|x - y|) dy = \int_0^1 \tilde{W}(|y|) dy, \quad \forall x \in [0, 1], \quad (2.12)$$

by the periodicity of  $W(|x - y|)$  induced by considering the argument modulo 1. Hence, the degree function  $\text{Deg}(x)$  is independent of  $x \in [0, 1]$ , which is the graphon analogue of a regular graph. A similar argument shows that for the induced deterministic graph we have  $\text{Deg}(A_d)$  is a constant multiple of the identity, thus making it a degree-uniform graph. The Erdős–Réyni and small-world graphons lead to ring networks, while the bipartite graphon does not. We note however that the degree function for the bipartite graph is also independent of  $x$  when  $\alpha = \frac{1}{2}$ , and the methods in the following section can easily be applied here as well. Unfortunately, it is not apparent what the larger class of graphons that the bipartite graphons belong to that lead to the same results in the following subsections and we therefore restrict our attention to ring networks.

## 2.2 Deterministic Graphs

As an intermediate step to relating the spectral properties of the deterministic weighted graph Laplacian to the graphon Laplacian, we will define a step function graphon that interpolates the discrete domain of the graph to form a step function graphon. To this end we partition  $[0, 1]$  into  $N$  subintervals

$$I_1^{(N)} = \left[0, \frac{1}{N}\right), \quad I_2^{(N)} = \left[\frac{1}{N}, \frac{2}{N}\right), \quad \dots \quad I_N^{(N)} = \left[\frac{N-1}{N}, 1\right). \quad (2.13)$$

Let us now define a step function  $W_N : [0, 1]^2 \rightarrow [0, 1]$  by

$$W_N(x, y) = W\left(\frac{|i-j|}{N}\right) \quad \text{for } (x, y) \in I_i^{(N)} \times I_j^{(N)}. \quad (2.14)$$

It is important to note that  $W_N$  is itself a degree-uniform graphon for each  $N \geq 1$ , and so the associated graphon Laplacian, denoted  $\mathcal{L}_N$ , acts by

$$\mathcal{L}_N f(x) := \int_0^1 W_N(x, y) (f(y) - f(x)) dy, \quad \forall x \in [0, 1], \quad (2.15)$$

analogous to (2.2) above. The relationship between  $\mathcal{L}_N$  and  $L_d$  is made explicit with the following lemma.

**Lemma 2.2.** *For each  $N \geq 2$ ,  $\lambda \in \mathbb{R}$  is an eigenvalue of  $L_d : \mathbb{R}^N \rightarrow \mathbb{R}^N$  if and only if  $\lambda/N \in \mathbb{R}$  is an eigenvalue of  $\mathcal{L}_N : L^2 \rightarrow L^2$ .*

*Proof.* Throughout this proof we fix  $N \geq 2$ . Begin by assuming that  $(\lambda, v) \in \mathbb{R} \times \mathbb{R}^N$  is an eigenpair of  $L_d$ , i.e.  $L_d v = \lambda v$ . Then, define the step function

$$f_v(x) = \sum_{i=1}^N v_i \chi_{I_i}(x) \quad (2.16)$$

where  $v = [v_1, v_2, \dots, v_N]^T$  and  $\chi_{I_i}(x)$  is the characteristic function of the interval  $I_i$ . Clearly  $f_v$  is square integrable since it takes only finitely many values. Then, for each  $1 \leq i \leq N$  and  $x \in I_i$  we have

$$\begin{aligned} \mathcal{L}_N f_v(x) &= \int_0^1 W_N(x, y) (f_v(y) - f_v(x)) dy \\ &= \sum_{j=1}^N \frac{1}{N} W\left(\frac{|i-j|}{N}\right) (v_j - v_i) \\ &= \frac{1}{N} [L_d v]_i \\ &= \frac{\lambda}{N} v_i \\ &= \frac{\lambda}{N} f_v(x). \end{aligned} \quad (2.17)$$

Hence,  $(\lambda/N, f_v) \in \mathbb{R} \times L^2$  is an eigenpair of  $\mathcal{L}_N : L^2 \rightarrow L^2$ , proving the first direction.

Now let us assume that  $(\lambda, f) \in \mathbb{R} \times L^2$  is an eigenpair of  $\mathcal{L}_N : L^2 \rightarrow L^2$ . Then, for each  $1 \leq i \leq N$  and  $x \in I_i$  we have

$$\begin{aligned} \lambda f &= \mathcal{L}_N f(x) \\ &= \int_0^1 W_N(x, y) (f(y) - f(x)) \, dy \\ &= \sum_{j=1}^N W\left(\frac{|i-j|}{N}\right) \int_{I_j} f(y) \, dy - \frac{1}{N} \sum_{j=1}^N W\left(\frac{|i-j|}{N}\right) f(x). \end{aligned} \tag{2.18}$$

Rearranging the above expression gives

$$\left[ \lambda + \frac{1}{N} \sum_{j=1}^N W\left(\frac{|i-j|}{N}\right) \right] f(x) = \sum_{j=1}^N W\left(\frac{|i-j|}{N}\right) \int_{I_j} f(y) \, dy, \tag{2.19}$$

and since the right-hand-side is independent of  $x \in I_i$ , it follows that  $f(x)$  is constant on  $I_i$  for each  $1 \leq i \leq N$ . Therefore, there exists  $v_i \in \mathbb{R}$ ,  $i = 1, 2, \dots, N$ , such that

$$f(x) = \sum_{i=1}^N v_i \chi_{I_i}(x). \tag{2.20}$$

Defining  $v = [v_1, v_2, \dots, v_N]^T \in \mathbb{R}^N$ , it now follows from simply rearranging the equalities in (2.17) that  $(N\lambda, v) \in \mathbb{R} \times \mathbb{R}^N$  is an eigenpair of  $L_d : \mathbb{R}^N \rightarrow \mathbb{R}^N$ . This completes the proof.  $\square$

Lemma 2.2 shows that there is a one-to-one correspondence between the eigenvalues of  $\mathcal{L}_N$  and  $L_d$ . Therefore, our goal in the remainder of this section is to show that the spectrum of  $\mathcal{L}_N$  converges to the spectrum of  $\mathcal{L}_W$  as  $N \rightarrow \infty$ , allowing one to view the eigenvalues of  $\mathcal{L}_W$  as the limit of eigenvalues of  $L_d$  (after rescaling by  $1/N$ ). This will be achieved by showing that  $\mathcal{L}_N$  converges to  $\mathcal{L}_W$  in the  $L^2 \rightarrow L^2$  operator norm, which in turn gives the convergence of the spectra. We present the following lemma that allows one to estimate the distance between graphon Laplacians in the operator norm topology, for which our desired convergence result is a corollary.

**Lemma 2.3.** *Let  $W_1$  and  $W_2$  be graphons with associated graphon Laplacians  $\mathcal{L}_{W_1}$  and  $\mathcal{L}_{W_2}$ . Then,*

$$\|\mathcal{L}_{W_1} - \mathcal{L}_{W_2}\|_{2 \rightarrow 2} \leq \sqrt{2} \|W_1 - W_2\|_1^{1/2} + \|\text{Deg}(W_1) - \text{Deg}(W_2)\|_\infty. \tag{2.21}$$

*Proof.* Since  $\mathcal{L}_{W_1}$  and  $\mathcal{L}_{W_2}$  are linear operators, it follows that

$$\begin{aligned} (\mathcal{L}_{W_1} - \mathcal{L}_{W_2})f(x) &= \int_0^1 [W_1(x, y) - W_2(x, y)] (f(y) - f(x)) \, dy \\ &= \int_0^1 [W_1(x, y) - W_2(x, y)] f(y) \, dy - [\text{Deg}(W_1)(x) - \text{Deg}(W_2)(x)] f(x), \end{aligned} \tag{2.22}$$

for all  $x \in [0, 1]$ . Then, using Hölder's inequality we can find that for all  $f \in L^\infty$  we have

$$\left\| \int_0^1 [W_1(x, y) - W_2(x, y)] f(y) \, dy \right\| \leq \|W_1 - W_2\|_1 \|f\|_\infty. \tag{2.23}$$



Hence, denoting the linear operator  $f \mapsto \int_0^1 [W_1(x, y) - W_2(x, y)]f(y)dy$  by  $T$  gives the operator norm bound  $\|T\|_{\infty \rightarrow 1} \leq \|W_1 - W_2\|_1$ . From [20, Lemma E.6] we get

$$\|T\|_{2 \rightarrow 2} \leq \sqrt{2}\|T\|_{\infty \rightarrow 1}^{1/2} \leq \sqrt{2}\|W_1 - W_2\|_1^{1/2}. \quad (2.24)$$

Then, for all  $f \in L^2$  we have that

$$\begin{aligned} \|(\mathcal{L}_{W_1} - \mathcal{L}_{W_2})f\|_2 &\leq \|Tf\|_2 + \|\text{Deg}(W_1) - \text{Deg}(W_2)\|f\|_2 \\ &\leq \sqrt{2}\|W_1 - W_2\|_1^{1/2}\|f\|_2 + \left( \int_0^1 |\text{Deg}(W_1)(x) - \text{Deg}(W_2)(x)|^2 |f(x)|^2 dx \right)^{\frac{1}{2}} \\ &\leq \sqrt{2}\|W_1 - W_2\|_1^{1/2}\|f\|_2 + \|\text{Deg}(W_1) - \text{Deg}(W_2)\|_{\infty} \left( \int_0^1 |f(x)|^2 dx \right)^{\frac{1}{2}} \\ &= \left( \sqrt{2}\|W_1 - W_2\|_1^{1/2} + \|\text{Deg}(W_1) - \text{Deg}(W_2)\|_{\infty} \right) \|f\|_2. \end{aligned} \quad (2.25)$$

This therefore gives the desired result.  $\square$

We immediately arrive at the following corollary that says that  $\mathcal{L}_N$ , defined in (2.15), converges in the  $L^2 \rightarrow L^2$  operator norm to  $\mathcal{L}_W$ , for any ring graphon  $W$ . As one will see in the following proof, in the case of general graphons  $W(x, y)$  we require that  $\text{Deg}(W_N) \rightarrow \text{Deg}(W)$  in the  $L^\infty$  norm, which may not always be the case. We do point out that bipartite graphons do in fact satisfy this property since the resulting degree matrices are piecewise constant, leading to the belief that the class of graphons that our results apply to is significantly larger than just the ring networks considered in this work.

**Corollary 2.4.** *Let  $W$  be a graphon and  $W_N$  defined from  $W$  as in (2.14). Then the associated graphon Laplacians  $\mathcal{L}_W$  and  $\mathcal{L}_N$  satisfy  $\|\mathcal{L}_W - \mathcal{L}_N\|_{2 \rightarrow 2} \rightarrow 0$  as  $N \rightarrow \infty$ .*

*Proof.* By construction of  $W_N$  we have  $W_N(x, y) \rightarrow W(x, y)$  as  $N \rightarrow \infty$  for every point of continuity  $(x, y)$  of  $W(x, y)$ . By assumption  $W$  is continuous almost-everywhere, and so we have pointwise convergence of  $W_N$  to  $W$  almost-everywhere. Since  $0 \leq W \leq 1$ , it follows from the dominated convergence theorem that  $\|W - W_N\|_1 \rightarrow 0$  as  $N \rightarrow \infty$ . Furthermore, the associated degree functions  $\text{Deg}(W)(x)$  and  $\text{Deg}(W_N)(x)$  are independent of  $x$ , so

$$\begin{aligned} \|\text{Deg}(W) - \text{Deg}(W_N)\|_{\infty} &= |\text{Deg}(W)(x) - \text{Deg}(W_N)(x)| \\ &= \left| \int_0^1 [W(x, y) - W_N(x, y)] dy \right| \\ &= \int_0^1 \left| \int_0^1 [W(x, y) - W_N(x, y)] dy \right| dx \\ &\leq \int_0^1 \int_0^1 |W(x, y) - W_N(x, y)| dy dx \\ &= \|W - W_N\|_1. \end{aligned} \quad (2.26)$$

Then, using Lemma 2.3 we have

$$\|\mathcal{L}_W - \mathcal{L}_N\|_{2 \rightarrow 2} \leq 2\|W - W_N\|_1^{1/2} + \|\text{Deg}(W) - \text{Deg}(W_N)\|_{\infty} \leq 2\|W - W_N\|_1^{1/2} + \|W - W_N\|_1, \quad (2.27)$$

thus giving that  $\|\mathcal{L}_W - \mathcal{L}_N\|_{2 \rightarrow 2} \rightarrow 0$  as  $N \rightarrow \infty$ , completing the proof.  $\square$

Corollary 2.4 is significant because if  $\lambda$  is an isolated eigenvalue of  $\mathcal{L}_W$  with finite multiplicity, it follows that for each associated eigenvector  $f \in L^2$  there exists a sequence of eigenpairs  $(\lambda_N, f_N) \in \mathbb{R} \times L^2$  of  $\mathcal{L}_N$  for each  $N \geq 2$  converging to  $(\lambda, f)$ . Furthermore, from Lemma 2.17, the sequence  $(\lambda_N, f_N)$  corresponds to a sequence of eigenpairs  $(N\lambda_N, v_N) \in \mathbb{R} \times \mathbb{R}^N$  to  $L_d$ .

### 2.3 Random Graphs

In the previous subsection we were able to show that the eigenvalues of the deterministic graph Laplacian limit as  $N \rightarrow \infty$  to the spectrum of the graphon Laplacian, after weighting by a factor of  $\frac{1}{N}$ . In this section our goal is to demonstrate the convergence of the eigenvalues and eigenvectors of  $L_r$  to the eigenvalues and eigenvectors of  $L_d$  with overwhelming probability. Our main result stating this fact is summarized in Theorem 2.7 below. The main technical hurdle is to show the convergence of the eigenvectors for large  $N$  since we do not have pointwise convergence of the elements in the matrices  $L_d$  and  $L_r$  for arbitrary graphons  $W$ , and so this precludes applying the Davis–Kahan theorem [13] which is the traditional tool used to demonstrate eigenvector convergence. We will circumvent this using the results of [44] which replaces the Frobenius norm (Euclidean norm of the elements of a matrix) with a matrix operator norm, defined for a matrix  $M$  by

$$\|M\| := \sup_{\|x\|_2=1} \|Mx\|_2, \quad (2.28)$$

where  $\|\cdot\|_2$  for a finite dimensional vector is simply the Euclidean norm. We refrain from including the subscript  $2 \rightarrow 2$  for matrix norms since we will not consider any other domains and ranges.

We will begin by bounding  $\|L_r - L_d\|$  with overwhelming probability. The following lemma is an extension of [37, Theorem 3.1] to combinatorial graph Laplacians since the aforementioned result only applies to adjacency matrices and normalized Laplacians. Although we suspect that an extension of these results to combinatorial graph Laplacians may be known in the literature, an appropriate reference could not be found and so we provide a detailed proof here.

**Lemma 2.5.** *Let  $N \geq 2$  and consider the graph Laplacians  $L_d$  and  $L_r$  as defined in (2.7) and (2.9), respectively. For all  $\varepsilon \in (0, \frac{1}{2})$ , there exists a constant  $C = C(\varepsilon)$ , independent of  $N$ , such that*

$$\mathbb{P}(\|L_r - L_d\| \geq N^{\frac{1}{2}+\varepsilon}) \leq 2Ne^{-CN^{2\varepsilon}}. \quad (2.29)$$

The main tool for proving Lemma 2.5 will be Corollary 7.1 from [37], which we state here as a lemma for the reader.

**Lemma 2.6** ([37], Corollary 7.1). *Let  $X_1, \dots, X_n \in \mathbb{C}^{d \times d}$  be mean-zero independent random Hermitian matrices and that there exists a  $M > 0$  with  $\|X_i\| \leq M$  almost surely for all  $1 \leq i \leq n$ . Define:*

$$\sigma^2 := \lambda_{\max} \left( \sum_{i=1}^n \mathbb{E}[X_i^2] \right). \quad (2.30)$$

*Then for all  $t \geq 0$ ,*

$$\mathbb{P} \left( \left\| \sum_{i=1}^n X_i \right\| \geq t \right) \leq 2de^{-\frac{t^2}{8\sigma^2+4Mt}}. \quad (2.31)$$

*Proof of Lemma 2.5.* For a given graphon  $W$  and a fixed  $N \geq 2$ , let us write  $p_{i,j} = W(\frac{i}{N}, \frac{j}{N})$  for  $i \neq j$  and  $p_{i,i} = 0$  if  $i = j$ . Hence, the adjacency matrices can be written

$$A_d = [p_{i,j}]_{1 \leq i,j \leq N} \quad (2.32)$$

and

$$A_r = [\xi_{i,j}]_{1 \leq i,j \leq N}, \quad \text{with} \quad \begin{cases} \mathbb{P}(\xi_{i,j} = 1) = 1 - \mathbb{P}(\xi_{i,j} = 0) = p_{i,j} & i \neq j \\ \xi_{i,i} = 0 & i = j \end{cases}. \quad (2.33)$$

Importantly,  $A_d = \mathbb{E}[A_r]$  and similarly  $L_d = \mathbb{E}[L_r]$ .

Let  $\{e_i\}_{i=1}^N$  be the canonical basis for  $\mathbb{R}^N$ . For each  $1 \leq i \leq j \leq N$  define the matrices  $B_{i,j} \in \mathbb{R}^{N \times N}$  by

$$B_{i,j} = \begin{cases} e_i e_j^T + e_j e_i^T, & i \neq j \\ e_i e_i^T, & i = j \end{cases}. \quad (2.34)$$

Note that  $B_{i,j}$  are real-valued, symmetric matrices and that the adjacency matrices can be written

$$\begin{aligned} A_d &= \sum_{1 \leq i \leq j \leq N} p_{i,j} B_{i,j}, \\ A_r &= \sum_{1 \leq i \leq j \leq N} \xi_{i,j} B_{i,j}. \end{aligned} \quad (2.35)$$

Consequentially, the associated graph Laplacians can be written

$$\begin{aligned} L_d &= \sum_{1 \leq i \leq j \leq N} p_{i,j} (B_{i,j} - B_{i,i} - B_{j,j}), \\ L_r &= \sum_{1 \leq i \leq j \leq N} \xi_{i,j} (B_{i,j} - B_{i,i} - B_{j,j}). \end{aligned} \quad (2.36)$$

Defining

$$X_{i,j} = (\xi_{i,j} - p_{i,j})(B_{i,j} - B_{i,i} - B_{j,j}) \quad (2.37)$$

gives that

$$L_r - L_d = \sum_{1 \leq i \leq j \leq N} (\xi_{i,j} - p_{i,j})(B_{i,j} - B_{i,i} - B_{j,j}) = \sum_{1 \leq i \leq j \leq N} X_{i,j}. \quad (2.38)$$

The matrices  $X_{i,j} \in \mathbb{R}^{N \times N}$  are independent, symmetric, and have mean zero. Furthermore, since each row of  $X_{i,j}$  has at most two nonzero entries that add to zero, it follows that

$$\|X_{i,j}\| \leq 2(\xi_{i,j} - p_{i,j}) \leq 2 \quad (2.39)$$

for every  $1 \leq i \leq j \leq N$ .

Now,

$$\begin{aligned} X_{i,j}^2 &= (\xi_{i,j} - p_{i,j})^2 (B_{i,j} - B_{i,i} - B_{j,j})^2 \\ &= (\xi_{i,j} - p_{i,j})^2 (B_{i,j}^2 + B_{i,i}^2 + B_{j,j}^2 - B_{i,j} B_{i,i} - B_{i,i} B_{i,j} - B_{i,j} B_{j,j} - B_{j,j} B_{i,j} + B_{i,i} B_{j,j} + B_{j,j} B_{i,i}). \end{aligned} \quad (2.40)$$

From the definition of the  $B_{i,j}$ , we have the following properties:

- (i)  $B_{i,i}B_{j,j} = 0$  for all  $i \neq j$ .
- (ii)  $B_{i,i}^2 = B_{i,i}$  for all  $1 \leq i \leq N$ .
- (iii)  $B_{i,j}^2 = B_{i,i} + B_{j,j}$  for all  $1 \leq i \leq j \leq N$ .
- (iv)  $B_{i,j}B_{i,i} + B_{i,i}B_{i,j} = B_{i,j}$  and  $B_{i,j}B_{j,j} + B_{j,j}B_{i,j} = B_{i,j}$  for all  $1 \leq i \leq j \leq N$ .

These properties can in turn be used to simplify (2.40), giving

$$\begin{aligned} X_{i,j}^2 &= (\xi_{i,j} - p_{i,j})^2(2B_{i,i} + 2B_{j,j} - 2B_{i,j}) \\ &= 2(\xi_{i,j} - p_{i,j})^2(B_{i,i} + B_{j,j} - B_{i,j}). \end{aligned} \quad (2.41)$$

Since the  $\xi_{i,j}$  are binary random variables, we have the expectation

$$\begin{aligned} \mathbb{E}[X_{i,j}^2] &= \underbrace{2p_{i,j}(1 - p_{i,j})^2(B_{i,i} + B_{j,j} - B_{i,j})}_{\xi_{i,j}=1} + \underbrace{2(1 - p_{i,j})p_{i,j}^2(B_{i,i} + B_{j,j} - B_{i,j})}_{\xi_{i,j}=0} \\ &= 2p_{i,j}(1 - p_{i,j})(B_{i,i} + B_{j,j} - B_{i,j}). \end{aligned} \quad (2.42)$$

Taking the sum over all  $1 \leq i \leq j \leq N$  gives

$$\sum_{1 \leq i \leq j \leq N} \mathbb{E}[X_{i,j}^2] = \sum_{1 \leq i \leq j \leq N} 2p_{i,j}(1 - p_{i,j})(B_{i,i} + B_{j,j} - B_{i,j}), \quad (2.43)$$

which is the negative of a graph Laplacian with edge weights between vertices  $i/N$  and  $j/N$  given by  $2p_{i,j}(1 - p_{i,j})$ . Therefore, from the Gershgorin circle theorem we have

$$\lambda_{\max} \left( \sum_{1 \leq i \leq j \leq N} \mathbb{E}[X_{i,j}^2] \right) \leq 2 \max_{1 \leq i \leq N} \sum_{j \neq i} 2p_{i,j}(1 - p_{i,j}) \leq 4(N - 1), \quad (2.44)$$

since  $0 \leq p_{i,j}(1 - p_{i,j}) \leq 1$  for all  $i \leq j$ .

We may now apply Lemma 2.6 with  $M = 2$  and  $\sigma^2 = 4(N - 1)$  to find that for all  $t > 0$  we have

$$\mathbb{P} \left( \left\| \sum_{1 \leq i \leq j \leq N} X_{i,j} \right\| \geq t \right) \leq 2Ne^{-\frac{t^2}{32N+8t-32}}. \quad (2.45)$$

For any  $\varepsilon > 0$ , take  $t = N^{\frac{1}{2}+\varepsilon}$ . Recalling from (2.38) that  $L_r - L_d = \sum_{1 \leq i \leq j \leq N} X_{i,j}$ , we therefore have

$$\mathbb{P} \left( \|L_r - L_d\| \geq N^{\frac{1}{2}+\varepsilon} \right) \leq 2Ne^{-\frac{N^{1+2\varepsilon}}{32N+8N^{1/2+\varepsilon}-32}} = 2Ne^{-\frac{N^{2\varepsilon}}{32+8N^{\varepsilon-1/2}-32N^{-1}}}. \quad (2.46)$$

Hence, for all  $\varepsilon \in (0, \frac{1}{2})$  we can bound the exponential bound above by  $e^{-C(\varepsilon)N^{2\varepsilon}}$  for some  $C(\varepsilon) > 0$  and all  $N \geq 2$ , thus giving the desired bound and completing the proof.  $\square$

Lemma 2.5 shows that as the number of vertices  $N$  increases, the operator norm of the difference between the deterministic graph Laplacian and the random graph Laplacian is no greater than  $N^{\frac{1}{2}+\varepsilon}$  with overwhelming probability, for all sufficiently small  $\varepsilon > 0$ . This now leads to the main result of this section.

**Theorem 2.7.** *Assume  $\mu \in \mathbb{R}$  is an isolated eigenvalue of  $\mathcal{L}_W$  with multiplicity  $1 \leq m < \infty$ . Then, for any  $\delta > 0$  sufficiently small and all  $N$  taken sufficiently large there are exactly  $m$  eigenvalues of  $L_d$ ,  $\lambda_1 \geq \lambda_2 \geq \dots \geq \lambda_m$ , and asymptotically almost surely exactly  $m$  eigenvalues of  $L_r$ ,  $\hat{\lambda}_1 \geq \hat{\lambda}_2 \geq \dots \geq \hat{\lambda}_m$ , such that*

$$\left| \frac{\lambda_k}{N} - \mu \right| < \delta, \quad \left| \frac{\hat{\lambda}_k}{N} - \mu \right| < \delta, \quad (2.47)$$

for all  $k = 1, \dots, m$ . Moreover, let  $V = [v_1, v_2, \dots, v_m] \in \mathbb{R}^{N \times m}$  and  $\hat{V} = [\hat{v}_1, \hat{v}_2, \dots, \hat{v}_m] \in \mathbb{R}^{N \times m}$  have orthonormal columns satisfying  $L_d v_k = \lambda_k v_k$  and  $L_r \hat{v}_k = \hat{\lambda}_k \hat{v}_k$  for  $k = 1, \dots, m$ . Then for each  $\varepsilon \in (0, \frac{1}{2})$ , with overwhelming probability there exists an orthonormal matrix  $\hat{O} \in \mathbb{R}^{m \times m}$  and a constant  $C > 0$  such that

$$\|\hat{V}\hat{O} - V\|_F \leq \frac{C}{N^{1/2-\varepsilon}} \quad (2.48)$$

where  $\|\cdot\|_F$  is the Frobenius matrix norm.

*Proof.* The existence of a  $\delta > 0$  and the  $m$  eigenvalues of  $L_d$  follow from our work in §2.2 on the convergence of the spectrum of this matrix to that of  $\mathcal{L}_W$ . Turning now to  $L_r$ , the results of Lemma 2.2 can be obtained through a nearly identical analysis for a  $\{0, 1\}$ -valued step function graphon defined analogously to  $W_N$  in (2.14) using the edge weights in  $L_r$ . This step function graphon converges with probability 1 to the graphon  $W$  in the so-called “cut-norm” [2, Lemma 2.5], which we refrain from defining here for brevity. Importantly, convergence of the step graphon coming from  $L_r$  to the graphon  $W$  in the cut norm gives convergence in the  $L^2 \rightarrow L^2$  operator norm by following [20, Lemma E.6]. Hence, asymptotically almost surely we have the analogous results from the deterministic Laplacian  $L_d$  for the spectrum of the random Laplacian  $L_r$  as  $N \rightarrow \infty$ . This verifies the claim that exactly  $m$  eigenvalues of  $L_r$  are coalescing near  $\mu$  after being divided by  $N$ , as  $N \rightarrow \infty$ .

Now, from this convergence and the fact that  $\mu$  is an isolated eigenvalue of  $\mathcal{L}_W$ , it follows there exists  $\eta > 0$  such that for each sufficiently large  $N$ , if  $\tilde{\lambda} \notin \{\lambda_1, \lambda_2, \dots, \lambda_m\}$  is an eigenvalue of  $L_d$ , then

$$\left| \frac{\tilde{\lambda}}{N} - \mu \right| > \eta. \quad (2.49)$$

By taking  $N$  large enough, we may take  $\eta > \delta > 0$ , and from the reverse triangle inequality we get

$$\left| \frac{\tilde{\lambda}}{N} - \frac{\lambda_j}{N} \right| \geq \left| \frac{\tilde{\lambda}}{N} - \mu \right| - \left| \frac{\lambda_j}{N} - \mu \right| > \eta - \delta \quad (2.50)$$

for all  $j = 1, \dots, m$ . Multiplying through by  $N$  implies that

$$|\tilde{\lambda} - \lambda_j| > (\eta - \delta)N \quad (2.51)$$

for all  $j = 1, \dots, m$ ,  $\tilde{\lambda} \notin \{\lambda_1, \lambda_2, \dots, \lambda_m\}$  an eigenvalue of  $L_d$ ,  $\eta > \delta > 0$  fixed, and all  $N$  sufficiently large. That is, the gap between the  $m$  eigenvalues  $\lambda_j$  of  $L_d$  and its other eigenvalues grows at a rate of  $\mathcal{O}(N)$  as  $N \rightarrow \infty$ .

Now, the variant of the Davis–Kahan theorem presented in [44, Theorem 2] gives that there exists an orthogonal matrix  $\hat{O} \in \mathbb{R}^{m \times m}$  such that

$$\|\hat{V}\hat{O} - V\|_F \leq \frac{\sqrt{8m}\|L_r - L_d\|}{\min\{|\tilde{\lambda} - \lambda_j|\}}, \quad (2.52)$$

where the minimum in the denominator is taken over all  $j = 1, \dots, m$  and  $\tilde{\lambda} \notin \{\lambda_1, \lambda_2, \dots, \lambda_m\}$  an eigenvalue of  $L_d$ . From Lemma 2.5 we have that for each  $\varepsilon \in (0, \frac{1}{2})$ , with overwhelming probability  $\|L_r - L_d\| \leq N^{1/2+\varepsilon}$ . Hence, with overwhelming probability we have

$$\|\hat{V}\hat{O} - V\|_F \leq \frac{\sqrt{8m}N^{1/2+\varepsilon}}{(\eta - \delta)N} = \frac{\sqrt{8m}}{(\eta - \delta)N^{1/2-\varepsilon}}, \quad (2.53)$$

thus proving the theorem.  $\square$

### 3 Turing Bifurcations for Ring Network Graphons

We now employ the machinery introduced in the previous section to understand Turing bifurcations for a natural class of ring networks wherein the weight of an edge in the network is a function of the distance between the two nodes. Graphons for ring networks have the property that they can be expressed as a Fourier Series

$$W(x, y) = \sum_{k \in \mathbb{Z}} c_k e^{2\pi i k(x-y)}, \quad (3.1)$$

for some  $c_k \in \mathbb{R}$  with  $c_k \rightarrow 0$  as  $|k| \rightarrow \infty$  for the  $L^2$  graphons considered here. This class of network models includes both the Erdős–Rényi and small-world models described in Example 2.1. An advantageous feature of this class of network models is that the eigenvalues of the corresponding graphon Laplacian  $\mathcal{L}_W$  are given explicitly in terms of the Fourier coefficients as  $\lambda_k = c_k - c_0$  with eigenfunctions  $e^{2\pi i k x}$ . Furthermore, since  $W$  is assumed to be real-valued and symmetric it follows that  $c_k = c_{-k}$ , and so  $\lambda_k = \lambda_{-k}$  for all  $k$ , meaning that non-zero eigenvalues come in pairs with (at least) two-dimensional eigenspaces spanned by  $e^{2\pi i k x}$  and its complex conjugate.

In this section, we consider the non-local graphon version of the Swift-Hohenberg equation,

$$\frac{du}{dt} = -(\mathcal{L}_W - \kappa)^2 u + \varepsilon u + r u^2 - b u^3 \quad (3.2)$$

for some constants  $r, b > 0$  and  $\kappa > 0$ . Recall that the parameter  $r$  controls the magnitude of the odd-symmetry breaking quadratic term while  $\kappa$  and  $\varepsilon$  control which mode(s)  $e^{2\pi i k x}$  are unstable. The linearization of the right-hand-side of (3.2) about the zero state,  $u = 0$ , with  $\varepsilon = 0$  is  $S_W = -(\mathcal{L}_W - \kappa)^2$  which is an operator on  $L^2$  with eigenvalues

$$\ell_k = -\lambda_k^2 + 2\kappa\lambda_k - \kappa^2. \quad (3.3)$$

If  $\kappa$  is fixed and it happens that  $\lambda_k = \kappa$  for some  $k$  then the zero state in (3.2) will become unstable for any  $\varepsilon > 0$  and we expect that a non-zero stationary solution will bifurcate. Our goal in this section is to employ center manifold theory to characterize the bifurcation that occurs as  $\varepsilon$  passes through zero. Since the eigenfunctions in this case are Fourier basis functions, the analysis will bear some resemblance to the case of Turing bifurcations that occur for PDEs with local spatial interactions coming from the spatial derivatives. In Section 3.1 that follows, we consider the case when a single pair of complex conjugate modes bifurcate and classify the bifurcation as a sub or supercritical pitchfork, depending on the choice of parameters. In contrast, we show in Section 3.2 that if the bifurcating eigenvalue is not simple then the resulting bifurcation may resemble a transcritical bifurcation, depending on whether there exists a resonance between the two bifurcating modes.

Prior to moving on to our analysis, we point out that many other bifurcation scenarios are possible beyond those that we cover in the following subsections. In such cases, bifurcating modes may or may not be in resonance and, depending on the particulars of their interactions, we could obtain center manifold reductions akin to those obtained in the following subsections. We do not pursue these calculations here as these further scenarios are not generic. Our intention with the the non-simple bifurcation scenario covered in Section 3.2 is simply to illustrate how the center manifold reductions would be carried out for these more complex scenarios and to demonstrate that the bifurcations are fundamentally different that the simple bifurcation case covered in Section 3.1.

Finally, a more exotic scenario can occur when the bifurcation involves the accumulation point at  $c_0$ , coming from the fact that  $\lambda_k \rightarrow c_0$  as  $|k| \rightarrow \infty$ . If  $\kappa = -c_0$  the bifurcation at  $\varepsilon = 0$  has infinite co-dimension and the methods of center manifold theory do not apply. Therefore, we are unable to classify the bifurcation rigorously in this scenario and leave it for a potential follow-up investigation. However, we will return to this case in Section 5 where we perform a numerical investigation from an eigenvalue of a random graph near the cluster point of the graphon Laplacian (after rescaling by the number of vertices).

### 3.1 Case I: Bifurcation through a single mode

In this section, we prove the following result that describes the bifurcation for a single mode. We recall throughout that  $\ell_k$  are given in (3.3) and correspond to the eigenvalues of the graphon Laplacian.

**Theorem 3.1.** *Fix  $\kappa > 0$  and suppose that there exists a  $k^* \in \mathbb{N}$  such that  $\ell_{k^*} = \ell_{-k^*} = 0$  while  $\ell_k < 0$  for all  $k \neq \pm k^*$ . Then for all  $|\varepsilon|$  sufficiently small (3.2) has an attracting two-dimensional center manifold in a neighborhood of  $u = 0$  and the flow restricted to this center manifold is topologically equivalent to the ordinary differential equations*

$$\begin{aligned} \frac{dw_{k^*}(t)}{dt} &= \varepsilon w_{k^*} - \left( 3b + \frac{4r^2}{\ell_0} + \frac{2r^2}{\ell_{2k^*}} \right) w_{k^*}^2 w_{-k^*} + \mathcal{O}(4) \\ \frac{dw_{-k^*}(t)}{dt} &= \varepsilon w_{-k^*} - \left( 3b + \frac{4r^2}{\ell_0} + \frac{2r^2}{\ell_{2k^*}} \right) w_{k^*} w_{-k^*}^2 + \mathcal{O}(4). \end{aligned} \quad (3.4)$$

If  $3b + 4\frac{r^2}{\ell_0} + 2\frac{r^2}{\ell_{2k^*}} > 0$ , then the bifurcation at  $\varepsilon = 0$  is supercritical and there exists an  $\varepsilon_0 > 0$  such that for all  $0 < \varepsilon < \varepsilon_0$  and  $\phi \in \mathbb{R}$  there exists a stationary solution  $u_{\varepsilon, \phi}$  of (3.2) with expansion

$$u_{\varepsilon, \phi}(x) = 2 \sqrt{\frac{\varepsilon}{3b + 4\frac{r^2}{\ell_0} + 2\frac{r^2}{\ell_{2k^*}}}} \cos(2\pi k^*(x - \phi)) + \mathcal{O}(\varepsilon). \quad (3.5)$$

On the other hand, if  $3b + 4\frac{r^2}{\ell_0} + 2\frac{r^2}{\ell_{2k^*}} < 0$  then the bifurcation is subcritical and a stationary solution of (3.2) of the form (3.5) exists for all  $-\varepsilon_0 < \varepsilon < 0$ .

*Proof.* The derivation of (3.4) is an application of the Center Manifold Theorem in infinite dimensions; see for example [17]. We begin with the eigenfunction expansion of a solution  $u(t, x)$  of (3.2) in the form

$$u(t, x) = \sum_{k \in \mathbb{Z}} w_k(t, \varepsilon) e^{2\pi i k x}. \quad (3.6)$$

Define the projection operator  $P_* : L^2 \rightarrow L^2$  by

$$P_*\phi = \langle \phi, e^{2\pi i k_* x} \rangle e^{2\pi i k_* x} + \langle \phi, e^{-2\pi i k_* x} \rangle e^{-2\pi i k_* x}, \quad (3.7)$$

where  $\langle \cdot, \cdot \rangle$  is the standard Hermitian inner product on the Hilbert space  $L^2$ . Since the range of  $P_*$  is finite-dimensional, it is closed, thus leading to the decomposition of  $u$  into  $u_* = P_*u$  and  $u_\perp = (I - P_*)u$ . Applying  $P_*$  and  $(I - P_*)$  to (3.2) results in the equations

$$\begin{aligned} \frac{du_*}{dt} &= \epsilon u_* + P_*(ru^2 - bu^3) \\ \frac{du_\perp}{dt} &= S_\perp u_\perp + \epsilon u_\perp + (I - P_*)(ru^2 - bu^3) \end{aligned} \quad (3.8)$$

where  $S_\perp$  is the restriction of  $\mathcal{L}_W$  onto the range of  $I - P_*$ . By assumption, the spectrum of  $S_\perp$  is bounded away from the imaginary axis, and therefore center manifold theory implies the existence of a local, flow-invariant center manifold parametrized as  $u_\perp = \Psi(u_*, \epsilon)$  [17]. The reduced flow on the two dimensional center manifold is then given by

$$\frac{du_*}{dt} = \epsilon u_* + P_*N(u_* + \Psi(u_*, \epsilon)), \quad (3.9)$$

after putting  $u_\perp = \Psi(u_*, \epsilon)$  into the first equation in (3.8) and letting the function  $N$  simply denote all nonlinear terms on the right-hand-side. To compute the reduced flow on the center manifold we therefore must obtain expansions for  $\Psi(u_*, \epsilon)$  and then expand the projection onto the center eigenspace in (3.9).

We now compute leading order nonlinear terms in  $N$  above. Using  $u_* = P_*u$  and the definition of  $P_*$  in (3.7), the equations for the critical bifurcating modes  $w_{k^*}$  and  $w_{-k^*}$  are

$$\begin{aligned} \frac{dw_{k^*}(t)}{dt} &= \epsilon w_{k^*} + r \sum_{k_1+k_2=k^*} w_{k_1} w_{k_2} - b \sum_{k_1+k_2+k_3=k^*} w_{k_1} w_{k_2} w_{k_3} \\ \frac{dw_{-k^*}(t)}{dt} &= \epsilon w_{-k^*} + r \sum_{k_1+k_2=-k^*} w_{k_1} w_{k_2} - b \sum_{k_1+k_2+k_3=-k^*} w_{k_1} w_{k_2} w_{k_3}. \end{aligned} \quad (3.10)$$

We now compute quadratic expansions for the graph of the center manifold. Using  $w_{k^*}$  and  $w_{-k^*}$  as coordinates on the center-manifold we can write the graph  $\Psi(u_*, \epsilon)$  using multi-index notation as

$$w_k = \sum_{|\alpha| \geq 2} \zeta_{k,\alpha} w_{k^*}^{\alpha_1} w_{-k^*}^{\alpha_2} \epsilon^{\alpha_3}, \quad (3.11)$$

where  $\alpha = (\alpha_1, \alpha_2, \alpha_3)$ . The expansions that are relevant for the computation of the leading order terms in the reduced flow on the center manifold are

$$\begin{aligned} w_0 &= \zeta_{0,(2,0,0)} w_{k^*}^2 + \zeta_{0,(1,1,0)} w_{k^*} w_{-k^*} + \zeta_{0,(0,2,0)} w_{-k^*}^2 + \mathcal{O}(3) \\ w_{\pm 2k^*} &= \zeta_{\pm 2k^*,(2,0,0)} w_{k^*}^2 + \zeta_{\pm 2k^*,(1,1,0)} w_{k^*} w_{-k^*} + \zeta_{\pm 2k^*,(0,2,0)} w_{-k^*}^2 + \mathcal{O}(3). \end{aligned} \quad (3.12)$$

To illustrate the computations, consider the equation for the homogeneous mode,

$$\frac{dw_0(t)}{dt} = \ell_0 w_0 + \epsilon w_0 + r \sum_{k_1+k_2=0} w_{k_1} w_{k_2} - b \sum_{k_1+k_2+k_3=0} w_{k_1} w_{k_2} w_{k_3}. \quad (3.13)$$



Substitute the expansion (3.12) and note that since the coefficients on  $w_{\pm k^*}^2$  are zero in (3.13) we have that  $\zeta_{0,(2,0,0)} = \zeta_{0,(0,2,0)} = 0$ . For the term involving  $w_{k^*}w_{-k^*}$ , after substituting (3.10) we consolidate the quadratic terms and find

$$\mathcal{O}(3) = \ell_0 \zeta_{0,(1,1,0)} w_{k^*} w_{-k^*} + 2r w_{k^*} w_{-k^*} + \mathcal{O}(3), \quad (3.14)$$

from which we obtain

$$\zeta_{0,(1,1)} = -\frac{2r}{\ell_0}. \quad (3.15)$$

A similar analysis obtains  $\zeta_{\pm 2k^*,(1,1,0)} = \zeta_{-2k^*,(2,0,0)} = \zeta_{2k^*,(0,2,0)} = 0$  and

$$\begin{aligned} \zeta_{2k^*,(2,0)} &= -\frac{r}{\ell_{2k^*}} \\ \zeta_{-2k^*,(0,2)} &= -\frac{r}{\ell_{2k^*}}. \end{aligned} \quad (3.16)$$

We then plug these expansions into (3.10), recalling that all  $w_k$  are quadratic in the center manifold coordinates  $w_{\pm k^*}$  and  $\varepsilon$ . Inspecting the terms in the summations, we see that the quadratic terms  $w_{k^*}^2$ ,  $w_{k^*}w_{-k^*}$  and  $w_{-k^*}^2$  are all absent and therefore owing to the quadratic dependence of the center manifold expansions we have that the nonlinearity for the reduced equation on the center manifold involves exclusively terms that are cubic order or higher. In the equation for  $w_{k^*}$ , one of these cubic terms comes from the interaction  $(k_1, k_2, k_3) = (k^*, k^*, -k^*)$  and after including all permutations of indices we obtain the  $-3b$  term in the center manifold reduction. Similar computations involving the quadratic interaction terms with  $(k_1, k_2) = (0, k^*)$  and  $(k_1, k_2) = (2k^*, -k^*)$  yield the remaining cubic terms in the center manifold expansion stated in (3.4).

Since  $u(x, t)$  is real, we have  $w_{k^*} = \overline{w_{-k^*}}$  and so letting  $w_{k^*}(t) = z(t)e^{-2\pi k^* i \phi}$  leads to a scalar bifurcation equation for  $z(t)$ ,

$$\frac{dz}{dt} = \varepsilon z - \left( 3b + 4\frac{r^2}{\ell_0} + 2\frac{r^2}{\ell_{2k^*}} \right) z^3 + \mathcal{O}(z\varepsilon^2, z^4). \quad (3.17)$$

Let

$$\Gamma := 3b + 4\frac{r^2}{\ell_0} + 2\frac{r^2}{\ell_{2k^*}}. \quad (3.18)$$

If  $\Gamma > 0$ , the implicit function theorem gives the existence of an equilibrium solution of (3.17), valid for sufficiently small  $\varepsilon > 0$ , with expansion

$$z_{\pm}(\varepsilon) = \pm \sqrt{\frac{\varepsilon}{\Gamma}} + \mathcal{O}(\varepsilon). \quad (3.19)$$

We see in this case that the resulting bifurcation is a supercritical pitchfork. Since  $z$  is an amplitude we consider only the root  $z_+(\varepsilon)$  and after reverting coordinates we obtain the result. If  $\Gamma < 0$  then the same formula holds but is valid only for  $\varepsilon < 0$  and the bifurcation is subcritical. This completes the proof.  $\square$

### 3.2 Case II: Bifurcation through repeated modes in resonance

Let us now consider the case when two modes simultaneously destabilize. This occurs when there exists a  $k_1$  and a  $k_2$  for which  $\ell_{k_1} = \ell_{-k_1} = \ell_{k_2} = \ell_{-k_2} = 0$ , as given in (3.3). In this subsection we will primarily focus on the case that the two modes are in 2 : 1 resonance, that is  $k_2 = 2k_1$ . The following result shows that this case leads to quadratic terms in the reduced equations on the center manifold.

**Theorem 3.2.** Suppose  $r \neq 0$  and suppose that for  $\kappa > 0$  fixed there exists a pair  $0 < k_1 < k_2$  such that  $\ell_{k_1} = \ell_{-k_1} = \ell_{k_2} = \ell_{-k_2} = 0$  and  $\ell_k < 0$  for all other  $k$ .

a) If  $k_2 = 2k_1$ , then, for  $|\varepsilon|$  sufficiently small there exists an attracting four dimensional center manifold in a neighborhood of  $u = 0$  whose dynamics are topologically conjugate to the ordinary differential equations

$$\begin{aligned}\frac{dw_{k_1}(t)}{dt} &= \varepsilon w_{k_1} + 2rw_{k_2}w_{-k_1} + \mathcal{O}(3) \\ \frac{dw_{-k_1}(t)}{dt} &= \varepsilon w_{-k_1} + 2rw_{-k_2}w_{k_1} + \mathcal{O}(3) \\ \frac{dw_{k_2}(t)}{dt} &= \varepsilon w_{k_2} + rw_{k_1}^2 + \mathcal{O}(3) \\ \frac{dw_{-k_2}(t)}{dt} &= \varepsilon w_{-k_2} + rw_{-k_1}^2 + \mathcal{O}(3).\end{aligned}\tag{3.20}$$

The resulting bifurcation leads to a pair of one-parameter bifurcating solutions with expansions

$$u_{\varepsilon, \phi, \pm}(x) = \pm \frac{\sqrt{2}\varepsilon}{r} \cos(2\pi \mathbf{i}(x - \phi)) - \frac{\varepsilon}{r} \cos(4\pi \mathbf{i}(x - \phi)) + \mathcal{O}(\varepsilon^2),\tag{3.21}$$

for any  $\phi \in \mathbb{R}$ .

b) If  $0 < k_1 < k_2$  and  $k_2 > 3k_1$  then for  $\varepsilon$  sufficiently small there exist an attracting four dimensional center manifold in a neighborhood of the origin. The center manifold dynamics decouple to cubic order and each pair  $w_{\pm k_1}$  and  $w_{\pm k_2}$  obey equations analogous to (3.4).

*Proof.* a) Let  $k_1 = k_*$ , so that  $k_2 = 2k_*$ . When  $\varepsilon = 0$ , by assumption the spectrum of the origin has four zero eigenvalues while the remainder are strictly negative. Once again, there exists a decomposition of  $u = u_* + u_\perp$  with  $u_* = P_*u$  and  $u_\perp = (I - P_*)u$  where  $P_*$  is the spectral projection onto the center eigenspace, spanned by  $e^{2\pi \mathbf{i}k_*x}$ ,  $e^{4\pi \mathbf{i}k_*x}$ , and their complex conjugates. The center manifold theorem again applies and we obtain the existence of a four dimensional attracting center manifold parameterized as  $u_\perp = \Psi(u_*, \varepsilon)$  [17]. The key point is that  $\Psi$  is quadratic in  $u_*$  to leading order. Therefore, the expansion of the graph of the center manifold will only come into play when computing the cubic terms and we can focus on the quadratic terms which only arise through interactions of the four bifurcating modes. Since  $2k_1 = k_2$  we obtain the quadratic term  $rw_{\pm k_1}^2$  in the equation for  $w_{\pm k_2}$  while  $k_2 - k_1 = k_1$  implies that the term  $2rw_{\pm k_2}w_{\mp k_1}$  appears in the equation for  $w_{\pm k_1}$ . We therefore obtain (3.20).

We now analyze the steady-states of (3.20). Since we are interested in real solutions it holds that  $w_{k_1} = \overline{w_{-k_1}}$  and  $w_{k_2} = \overline{w_{-k_2}}$ . Equilibrium solutions then satisfy the system of complex equations,

$$\begin{aligned}0 &= \varepsilon w_{k_1} + 2rw_{k_2}\overline{w_{k_1}} + \mathcal{O}(3) \\ 0 &= \varepsilon w_{k_2} + rw_{k_1}^2 + \mathcal{O}(3).\end{aligned}\tag{3.22}$$

Up to quadratic order, solutions to the second equation take the form  $w_2 = -\frac{\varepsilon}{r}w_{k_1}^2$ . Substituting into the first equation and again focusing exclusively on the quadratic terms solutions we have

$$\varepsilon w_{k_1} (\varepsilon^2 - 2r^2|w_{k_1}|^2) = 0.\tag{3.23}$$

Hence,

$$w_{k_1} = \eta e^{-2\pi \mathbf{i}\Omega}, \quad \eta = \frac{1}{\sqrt{2}} \left| \frac{\varepsilon}{r} \right|\tag{3.24}$$

and

$$w_{k_2} = \frac{-r}{\varepsilon} \eta^2 e^{-4\pi i \Omega} = -\frac{\varepsilon}{2r} e^{-4\pi i \Omega}, \quad (3.25)$$

for some  $\Omega \in \mathbb{R}$ . This leads to a pair of bifurcating solutions that have the expansions given in (3.21).

b) Since  $k_2 > 3k_1$  we find that the bifurcating modes do not interact under quadratic or cubic coupling. Therefore, for  $w_{\pm k_1}$  the only terms that are relevant in deducing the quadratic and cubic terms in the reduced equation on the center manifold are those involving  $w_{\pm k_1}$ ,  $w_{\pm 2k_1}$  and  $w_0$ , giving that the analysis follows as in the proof of Theorem 3.1. Likewise, the for  $w_{\pm k_2}$  the only terms that are relevant in deducing the quadratic and cubic terms in the reduced equation on the center manifold are those involving  $w_{\pm k_2}$ ,  $w_{\pm 2k_2}$  and  $w_0$  and, again, the reduced equations are (to cubic order) obtained in a manner analogous to those in Theorem 3.1. We omit the details.  $\square$

**Remark 3.3.** *Theorem 3.1 and Theorem 3.2 are not exhaustive. Other scenarios are possible: for example, when  $k_2 = 3k_1$  another cubic term arises in the reduced equations on the center manifold or for bifurcations with higher co-dimension and where the bifurcating modes may or may not be in resonance. In principal, the analysis presented here could be extended to those cases should an application necessitate it. The main takeaway from Theorem 3.2 is that resonant interaction of modes can lead to transcritical bifurcations, which we also expect for many of the more exotic scenarios that we outlined in this remark.*

*If we contrast with the case of the local Swift-Hohenberg PDE in one space dimension we note that it is not typically the case that the inclusion of quadratic terms will lead to the occurrence of a transcritical bifurcation. However, this is not so rare in higher dimensional problems. For example, quadratic terms can lead to a resonance between roll and hexagonal patterns for the planar Swift-Hohenberg PDE; see for example [12].*

*Coming back to the graphon operators considered here, we note that one could also be interested in the case where the bifurcation involves the accumulation point of the graphon Laplacian spectrum. Here the bifurcation has infinite codimension and the center manifold theorem is not sufficient to describe the resulting bifurcation.*

## 4 Turing Bifurcations on Random Graphs

In this section we study Turing bifurcations for the Swift-Hohenberg equation (1.1) defined on random graphs. We will consider random graphs of ring networks derived from a graphon  $W(x, y) = W(|x - y|)$  so that the probability of two nodes having an edge connecting them is a function of the distance between the two nodes. Based upon the results of Section 2 we expect that when the number of nodes  $N$  is sufficiently large then (isolated) eigenvalues and their eigenvectors of the random graph are well approximated by eigenvalues (after scaling) and eigenvectors of the deterministic nonlocal graphon operator, as is detailed in Theorem 2.7.

As was pointed out in Section 3, ring networks have the advantageous property that their graphons can be represented in terms of Fourier series and the graphon eigenvalues and eigenvectors are simply derived from the Fourier coefficients and corresponding Fourier basis functions. Since  $W$  is translationally invariant it holds that all eigenvalues aside from the homogeneous one generically have algebraic and geometric multiplicity two. In creating a random graph from the graphon this translational invariance is broken and so we expect generically that all eigenvalues of the matrix  $L_r$  are simple.

Our main result is the following, which is the random graph analog of Theorem 3.1.

**Theorem 4.1.** *Consider the graphon  $W(x, y) = \sum_k c_k e^{2\pi i k(x-y)}$  and assume that there exists a  $k^*$  such that  $\mu := c_{k^*} - c_0$  is an isolated eigenvalue of  $\mathcal{L}_W$  with minimal algebraic multiplicity of two and  $c_{2k^*} \neq 0$  so that  $c_{2k^*} - c_0$  is an eigenvalue of finite (even) algebraic multiplicity  $m$ . Then, for any  $\delta > 0$  sufficiently small, with high probability the constructed random graph on  $N \gg 1$  vertices according to the procedure in (2.8) with associated graph Laplacian  $L_r$  has an eigenvalue  $\lambda_1$  that satisfies*

$$\left| \frac{\lambda_1(L_r)}{N} - (c_{k^*} - c_0) \right| < \delta. \quad (4.1)$$

Furthermore, for  $\kappa = \lambda_1$  and  $|\varepsilon|$  sufficiently small, there exists  $\Omega \in \mathbb{R}$  such that (1.1) has a nontrivial pair of equilibrium solutions which may be expanded as

$$u_j = \sqrt{2} z_1^\pm(\varepsilon, \delta) \cos \left( 2\pi k^* \left( \frac{j-1}{N} - \Omega \right) \right) + \mathcal{O}(\varepsilon, \delta^2), \quad (4.2)$$

for some  $z_1^\pm(\varepsilon, \delta)$  defined in (4.22).

Prior to providing the proof, we comment on the condition that  $c_{2k^*} \neq 0$ . If we had  $c_{2k^*} = 0$ , then the eigenvalue  $c_{2k^*} - c_0$  lies at the accumulation point of the spectrum of  $\mathcal{L}_W$ . We would still be able to perform a center manifold reduction and obtain an equation analogous to (4.30) below, however, since Theorem 2.7 does not provide good control over the difference between the eigenvalues of  $L_r$  and those near at the accumulation point for the spectrum of  $\mathcal{L}_W$ , we do not have the means to predict the cubic coefficient on the one-dimensional center manifold based upon properties of the graphon alone. Therefore, this case is omitted since our analysis cannot be applied in this situation.

*Proof.* Let  $W(x, y) = \sum_k c_k e^{2\pi i k(x-y)}$  be the ring-network graphon and consider (1.1) with  $L = L_r$  and  $\kappa = \lambda_1$ . Our goal is to characterize the bifurcation occurring in (1.1) at  $\varepsilon = 0$  and to compare this bifurcation to the one that occurs in the nonlocal equation (2.3) with  $\kappa = \mu$ .

As a preliminary, we obtain required estimates on some eigenvectors and eigenvalues of  $L_r$ . From Theorem 2.7 we have that for any  $\delta > 0$  taken sufficiently small, if we let  $\lambda_k$  denote the first  $2 + m$  eigenvalues of  $L_r$  on  $N$  vertices, with high probability we have

$$\begin{aligned} \left| \frac{\lambda_{1,2}(L_r)}{N} - (c_{k^*} - c_0) \right| &< \delta \\ \left| \frac{\lambda_{3,4,\dots,2+m}(L_r)}{N} - (c_{2k^*} - c_0) \right| &< \delta. \end{aligned} \quad (4.3)$$

By Theorem 2.7, we can assume that with high probability the eigenvectors for  $L_r$  are  $\mathcal{O}(\delta)$  close to the eigenvectors of the deterministic graph  $L_d$ . In turn, by Corollary 2.4 we have that the deterministic eigenvectors can be related to the Fourier eigenfunctions of the graphon. Therefore, with high probability we have that the orthogonal eigenvectors of  $L_r$  satisfy

$$\begin{aligned} |v_{1,2} - a_{1,2}\omega_{k^*} - \overline{a_{1,2}}\omega_{-k^*}| &< \delta \\ \left| v_j - a_j\omega_{2k^*} - \overline{a_j}\omega_{-k^*} - \sum_{n=1}^{\frac{m}{2}-1} (b_{jn}\omega_{k_n} + \overline{b_{jn}}\omega_{k_n}) \right| &< \delta, \end{aligned} \quad (4.4)$$

for all  $j = 3, 4, \dots, 2 + m$ , for some coefficients  $a_k \in \mathbb{C}$ ,  $b_{jn} \in \mathbb{C}$  and where  $\omega_k$  are the normalized discrete Fourier basis vector

$$\omega_k = \frac{1}{\sqrt{N}} \left( e^{2\pi k i x_0}, e^{2\pi k i x_1}, \dots, e^{2\pi k i x_{N-1}} \right)^T. \quad (4.5)$$

By orthonormality of the eigenvectors  $v_k$  we also see that  $|a_1|^2 = \frac{1}{2} + \mathcal{O}(\delta)$ , or equivalently  $a_1 = \frac{1}{\sqrt{2}} e^{-2\pi i \Omega} + \mathcal{O}(\delta)$  for some  $\Omega \in \mathbb{R}$ . As a final preliminary, recall that zero is always an eigenvalue of the random graph Laplacian,  $L_r$ , and the associated eigenvector is constant. We denote this eigenvalue/eigenvector pair as  $(\lambda_N, v_N) = (0, \omega_0)$ .

Let us momentarily assume that  $m = 2$  so that  $c_{2k^*} - c_0$  is also an isolated eigenvalue of  $\mathcal{L}_W$  of (minimal) algebraic multiplicity two. We will return to the case of  $m > 2$  below. For  $m = 2$ , with high probability we have

$$\begin{aligned} |v_3 - a_3 \omega_{2k^*} - \bar{a}_3 \omega_{-2k^*}| &< \delta \\ |v_4 - a_4 \omega_{2k^*} - \bar{a}_4 \omega_{-2k^*}| &< \delta. \end{aligned} \quad (4.6)$$

Let  $v_5, v_6, \dots, v_{N-1}$  denote the remaining  $N - 5$  eigenvectors of  $L_r$ , which exist and are orthonormal since  $L_r$  is symmetric. It what follows we will assume that all high probability statements are true to avoid quantifying probabilistic statements throughout this proof. This will help ease the presentation of the results.

We now perform a center manifold reduction. To begin, expand the solution in its basis of eigenvectors as

$$u(t) = \sum_{k=1}^N w_k(t, \varepsilon) v_k. \quad (4.7)$$

This diagonalizes the linear part of (1.1) and converts it into the system of equations

$$\frac{dw_k}{dt} = l_k w_k + \varepsilon w_k + r Q_k(w) + C_k(w), \quad (4.8)$$

where we can write  $l_1 = 0$ ,  $l_2 = -\delta^2 N^2 \rho_2$ , and  $l_k = -N^2 \rho_k$ , with  $\rho_k > 0$  for all  $k > 1$  since  $c_{k^*} - c_0$  is an isolated eigenvalue of  $\mathcal{L}_W$  with algebraic multiplicity 2. Consequently, the origin in (4.8) has a one dimensional center manifold which can be written as a graph over the center eigenspace; namely  $w_k = H_k(w_1, \varepsilon)$ .

The quadratic terms in (4.8) can be computed by projecting  $u(t) \circ u(t)$  onto  $v_k$ , or via the formula

$$Q_k(w) = \left\langle v_k, \left( \sum_i w_i(t) v_i \right) \circ \left( \sum_j w_j(t) v_j \right) \right\rangle = \sum_{k_1, k_2} w_{k_1} w_{k_2} \langle v_k, v_{k_1} \circ v_{k_2} \rangle, \quad (4.9)$$

where we recall that  $\langle u, v \rangle$  is the Hermitian inner product and  $\circ$  denotes the Hadamard product.

Consider  $k = 1$ . We may use (4.4) and (4.6) to find

$$\sqrt{N} Q_1(w) = r \beta w_1^2 + 2r w_1 w_N + 2r q_{113} w_1 w_3 + 2r q_{114} w_1 w_4 + 2r q_{123} w_2 w_3 + 2r q_{124} w_2 w_4 + \delta \tilde{Q}_1(w), \quad (4.10)$$

where owing to the orthogonality of the discrete Fourier basis vectors we have

$$\beta = \sqrt{N} \langle v_1, v_1 \circ v_1 \rangle = \sqrt{N} \langle a_1 \omega_{k^*} + \bar{a}_1 \omega_{-k^*}, a_1^2 \omega_{2k^*} + 2a_1 \bar{a}_1 \omega_0 + \bar{a}_1^2 \omega_{-2k^*} \rangle + \mathcal{O}(\delta) = \mathcal{O}(\delta), \quad (4.11)$$

and

$$q_{113} = a_1^2 \bar{a}_3 + \bar{a}_1^2 a_3, \quad q_{114} = a_1^2 \bar{a}_4 + \bar{a}_1^2 a_4, \quad q_{123} = a_2^2 \bar{a}_3 + \bar{a}_2^2 a_3, \quad q_{124} = a_2^2 \bar{a}_4 + \bar{a}_2^2 a_4. \quad (4.12)$$

The cubic terms can be computed by the formula

$$C_k(w) = \left\langle v_k, \left( \sum_i w_i(t) v_i \right) \circ \left( \sum_j w_j(t) v_j \right) \circ \left( \sum_l w_l(t) v_l \right) \right\rangle = \sum_{k_1, k_2, k_3} w_{k_1} w_{k_2} w_{k_3} \langle v_k, v_{k_1} \circ v_{k_2} \circ v_{k_3} \rangle. \quad (4.13)$$

So, we have

$$\begin{aligned} \langle v_1, v_1 \circ v_1 \circ v_1 \rangle &= \frac{1}{N} \langle a_1 \omega_{k^*} + \bar{a}_1 \omega_{-k^*}, a_1^3 \omega_{3k^*} + 3a_1^2 \bar{a}_1 \omega_{k^*} + 3a_1 \bar{a}_1^2 \omega_{-k^*} + \bar{a}_1^3 \omega_{-3k^*} \rangle + \mathcal{O}(\delta) \\ &= \frac{1}{N} \langle a_1 \omega_{k^*} + \bar{a}_1 \omega_{-k^*}, 3a_1^2 \bar{a}_1 \omega_{k^*} + 3a_1 \bar{a}_1^2 \omega_{-k^*} \rangle + \mathcal{O}(\delta). \end{aligned} \quad (4.14)$$

Using  $|a_1|^2 = \frac{1}{2} + \mathcal{O}(\delta)$  therefore implies

$$C_1(w) = -\frac{3b}{2N} w_1^3 + \delta \tilde{C}_1(w, \delta). \quad (4.15)$$

We now have obtained the required expansions for the equation that governs  $w_1$  in (4.8). To compute the scalar ODE that describes the reduced equation on the center manifold we must express all  $w_k$ , for  $k \neq 1$  in terms of  $w_1$ . Recall the notation that the graph of the center manifold is denoted  $w_k = H_k(w_1, \varepsilon)$ . To obtain expansions valid to cubic order we will require quadratic expansions for these graphs for the components  $w_3$ ,  $w_4$  and  $w_N$ . These are computed as follows. Consider first the case of  $w_N$ . Expanding (4.8) and using (4.9) we can compute the quadratic term in the expansion of  $H_N(w_1, \varepsilon)$  by a normal form transformation where we find  $\zeta$  for which  $w_N = \zeta w_1^2$  satisfies (to leading order)

$$\frac{dw_N}{dt} = l_N w_N + \frac{r}{\sqrt{N}} w_1^2. \quad (4.16)$$

Thus,  $\zeta = -\frac{r}{\sqrt{N} l_N} + \mathcal{O}(\delta)$ . This procedure yields expansions for  $H_3$ ,  $H_4$  and  $H_N$  which end up being,

$$\begin{aligned} H_3(w_1, \varepsilon) &= -\frac{r (a_3 \bar{a}_1^2 + \bar{a}_3 a_1^2)}{\sqrt{N} l_3} w_1^2 + \mathcal{O}(w_1^3 + \varepsilon w_1^2) + \mathcal{O}(\delta) \\ H_4(w_1, \varepsilon) &= -\frac{r (a_4 \bar{a}_1^2 + \bar{a}_4 a_1^2)}{\sqrt{N} l_4} w_1^2 + \mathcal{O}(w_1^3 + \varepsilon w_1^2) + \mathcal{O}(\delta) \\ H_N(w_1, \varepsilon) &= -\frac{r}{\sqrt{N} l_N} w_1^2 + \mathcal{O}(w_1^3 + \varepsilon w_1^2) + \mathcal{O}(\delta). \end{aligned} \quad (4.17)$$

With these expansions, we may now compute a reduced flow in the center manifold. We find

$$\frac{dw_1}{dt} = \varepsilon w_1 + \frac{r\beta}{\sqrt{N}} w_1^2 - \frac{1}{N} \left( \frac{3b}{2} + \frac{2r^2}{l_N} + \frac{2r^2 q_{113}^2}{l_3} + \frac{2r^2 q_{114}^2}{l_4} \right) w_1^3 + \mathcal{O}(w_1^4 + \varepsilon w_1^3 + \delta w_1^3 + \delta^2 w_1^2). \quad (4.18)$$

The cubic terms can be simplified by noting that orthogonality of the eigenvectors  $v_k$  implies that  $a_k \bar{a}_j + a_j \bar{a}_k = \mathcal{O}(\delta)$  for all  $k \neq j$  while normality implies  $a_k \bar{a}_k = \frac{1}{2} + \mathcal{O}(\delta)$ . Taken all together these facts imply that  $a_3^2 + \bar{a}_3^2 = \mathcal{O}(\delta)$  and hence

$$q_{113}^2 + q_{114}^2 = a_1^4 (\bar{a}_3^2 + \bar{a}_4^2) + 2|a_1|^4 (|a_3|^2 + |a_4|^2) + \bar{a}_1^4 (a_3^2 + a_4^2) = \frac{1}{2} + \mathcal{O}(\delta). \quad (4.19)$$

Finally, since  $|l_3 - l_4| = \mathcal{O}(\delta)$  we have then reduced (4.18) to

$$\frac{dw_1}{dt} = \varepsilon w_1 + \frac{r\beta}{\sqrt{N}} w_1^2 - \frac{1}{N} \left( \frac{3b}{2} + \frac{2r^2}{l_N} + \frac{r^2}{l_3} \right) w_1^3 + \mathcal{O}(w_1^4 + \varepsilon w_1^3 + \delta w_1^3 + \delta^2 w_1^2), \quad (4.20)$$

which constitutes the leading order expansion of the center manifold of (1.1) near  $(u, \varepsilon) = (0, 0)$ .

To obtain steady-state solutions on the center manifold, begin by letting  $w_1 = \sqrt{N} z_1$ . Then (4.20) is transformed to

$$\frac{dz_1}{dt} = \varepsilon z_1 + r\beta z_1^2 - \left( \frac{3b}{2} + \frac{2r^2}{l_N} + \frac{r^2}{l_3} \right) z_1^3 + \mathcal{O}(z_1^4 + \varepsilon z_1^3 + \delta z_1^3). \quad (4.21)$$

Applying the implicit function theorem we find that for  $\varepsilon$  and  $\delta$  sufficiently small there exists a pair of equilibrium points

$$z_1^\pm(\varepsilon, \delta) = \frac{\beta r}{2\Gamma_r} \pm \frac{1}{2\Gamma_r} \sqrt{\beta^2 r^2 + 4\Gamma_r \varepsilon} + \mathcal{O}(\varepsilon, \delta^2), \quad (4.22)$$

where

$$\Gamma_r = \frac{3b}{2} + \frac{2r^2}{l_N} + \frac{r^2}{l_3} \quad (4.23)$$

is the cubic coefficient on the center manifold. For any  $\delta \neq 0$  the bifurcation occurring near the zero state is transcritical, while if  $\delta$  is close to zero it is accompanied by a saddle node bifurcation occurring at

$$\varepsilon_{SN} \approx -\frac{\beta^2 r^2}{4\Gamma_r}. \quad (4.24)$$

The sign of  $\Gamma_r$  determines whether the equilibrium  $z_1^\pm(\varepsilon, \delta)$  exist for  $\varepsilon > \varepsilon_{SN}$  ( $\Gamma_r > 0$ ) or for  $\varepsilon < \varepsilon_{SN}$  ( $\Gamma_r < 0$ ). We now revert to the original coordinates of (1.1).

Reverting coordinates back to those of (1.1) we have the existence of a bifurcating solution of the form

$$u_j = \frac{2}{\sqrt{2}} z_1^\pm(\varepsilon, \delta) \cos \left( 2\pi k^* \left( \frac{j-1}{N} + \Omega \right) \right) + \mathcal{O}(\varepsilon, \delta^2), \quad (4.25)$$

for  $\Omega$  defined above.

The preceding analysis assumed that  $c_{2k^*} - c_0$  is an isolated eigenvalue of  $\mathcal{L}_W$  of minimal multiplicity two. We now consider the situation where this eigenvalue remains isolated but has multiplicity  $m > 2$  so that the expansions (4.4) hold, i.e

$$v_j = a_j \omega_{2k^*} + \bar{a}_j \omega_{-2k^*} + \sum_{n=1}^{\frac{m}{2}-1} (b_{jn} \omega_{k_n} + \bar{b}_{jn} \omega_{k_n}) + \delta p_j, \quad 3 \leq j \leq 3+m, \quad (4.26)$$

for some nonzero  $k_n \neq k^*$ . Orthonormality of the eigenvectors implies that

$$\sum_{j=3}^{3+m} a_j \bar{a}_j = 1 + \mathcal{O}(\delta), \quad \sum_{j=3}^{3+m} a_j^2 = \mathcal{O}(\delta), \quad (4.27)$$

and so we can generalize (4.8) to this case and obtain

$$\sqrt{N} Q_1(w) = r\beta w_1^2 + 2r w_1 w_N + 2r \sum_{j=3}^{3+m} (q_{11j} w_1 w_j + q_{12j} w_2 w_j) + \delta \tilde{Q}_1(w), \quad (4.28)$$

where  $q_{11j} = a_j \bar{a}_1^2 + \bar{a}_j a_1^2$ . Repeating the analysis above, we find expansions for the graph defining the center manifold as

$$\begin{aligned} H_j(w_1, \varepsilon) &= -\frac{r q_{11j}}{\sqrt{N} l_j} w_1^2 + \mathcal{O}(w_1^3 + \varepsilon w_1^2), \quad 3 \leq j \leq 3 + m \\ H_N(w_1, \varepsilon) &= -\frac{r}{\sqrt{N} l_N} w_1^2 + \mathcal{O}(w_1^3 + \varepsilon w_1^2). \end{aligned} \quad (4.29)$$

We then compute the reduced equation on the center manifold to obtain, in analogy with (4.18),

$$\frac{dw_1}{dt} = \varepsilon w_1 + \frac{r\beta}{\sqrt{N}} w_1^2 - \frac{1}{N} \left( \frac{3b}{2} + \frac{2r^2}{l_N} + \sum_{j=3}^{3+m} \frac{2r^2 q_{11j}^2}{l_j} \right) w_1^3 + \mathcal{O}(w_1^4 + \varepsilon w_1^3 + \delta w_1^3 + \delta^2 w_1^2). \quad (4.30)$$

Employing (4.27) this reduces to

$$\frac{dw_1}{dt} = \varepsilon w_1 + \frac{r\beta}{\sqrt{N}} w_1^2 - \frac{1}{N} \left( \frac{3b}{2} + \frac{2r^2}{l_N} + \frac{r^2}{l_3} \right) w_1^3 + \mathcal{O}(w_1^4 + \varepsilon w_1^3 + \delta w_1^3 + \delta^2 w_1^2).$$

which has the identical form to the previous case seen in (4.20). This completes the proof.  $\square$

**Remark 4.2.** A direct link between the bifurcation equation obtained for the random graph in (4.21) and that of the non-local graphon model (3.17) could be obtained by an  $N$ -dependent rescaling of coefficients. If we re-scale parameters by  $\varepsilon = \tilde{\varepsilon} N^2$ ,  $r = \tilde{r} N^2$ ,  $b = \tilde{b} N^2$ , re-scale  $z_1 = \sqrt{2} \tilde{z}_1$  and re-scale the dependent variable by  $t = \tau N^{-2}$  then (4.21) is transformed to

$$\frac{d\tilde{z}_1}{d\tau} = \tilde{\varepsilon} \tilde{z}_1 + \sqrt{2} \tilde{r} \beta \tilde{z}_1^2 - \left( 3\tilde{b} + \frac{4\tilde{r}^2}{\ell_0} + \frac{2\tilde{r}^2}{\ell_{2k^*}} \right) \tilde{z}_1^3 + \mathcal{O}(\tilde{z}_1^4 + \varepsilon \tilde{z}_1^3 + \delta \tilde{z}_1^3). \quad (4.31)$$

We now present the analogous result to Theorem 4.1 for the case when the graphon Laplacian has bifurcating modes that are in 2 : 1 resonance. We show that these bifurcations manifest as transcritical bifurcations in (1.1) which stem from resonant graphon eigenvalues.

**Theorem 4.3.** Consider the graphon  $W(x, y) = \sum_k c_k e^{2\pi i k(x-y)}$  and assume that there exists a  $k^*$  such that  $c_{k^*} = c_{2k^*}$  and  $\mu := c_{k^*} - c_0$  is an isolated eigenvalue of  $\mathcal{L}_W$  with minimal algebraic multiplicity of four. Then, for any  $\delta > 0$  sufficiently small, with high probability the constructed random graph on  $N \gg 1$  vertices according to the procedure in (2.8) with associated graph Laplacian  $L_r$  has an eigenvalue  $\lambda_1$  that satisfies

$$\left| \frac{\lambda_1(L_r)}{N} - (c_{k^*} - c_0) \right| < \delta. \quad (4.32)$$

Furthermore, for  $\kappa = \lambda_1$  and  $|\varepsilon|$  sufficiently small, there exists  $\Omega_{1,2} \in \mathbb{R}$  and  $\eta_{1,2} > 0$  such that (1.1) has a nontrivial equilibrium solution which may be expanded as

$$u_j = \varepsilon \eta_1 \cos \left( 2\pi k^* \left( \frac{j-1}{N} - \Omega_1 \right) \right) + \varepsilon \eta_2 \cos \left( 4\pi k^* \left( \frac{j-1}{N} - \Omega_2 \right) \right) + \mathcal{O}(\varepsilon^2, \delta^2). \quad (4.33)$$

*Proof.* The proof proceeds similarly to that of Theorem 4.1 and so we only highlight the differences here. Suppose the same set up as in Theorem 4.1, except we assume that the graphon eigenvalue has multiplicity



four and the bifurcating modes are  $e^{2\pi i k^* x}$  and  $e^{4\pi i k^* x}$ . From Theorem 2.7 we have that for any  $\delta > 0$  taken sufficiently small, with high probability there exists an eigenvalue,  $\lambda_1$ , of  $L_r$  with  $N$  vertices such that

$$\left| \frac{\lambda_1(L_r)}{N} - (c_{k^*} - c_0) \right| < \delta. \quad (4.34)$$

Moreover, with high probability the corresponding eigenvector satisfies,

$$|v_1 - v_3 - a_1 \omega_{k^*} - \bar{a}_1 \omega_{-k^*} - a_2 \omega_{2k^*} - \bar{a}_2 \omega_{-2k^*}| < \delta, \quad (4.35)$$

for some coefficients  $a_{1,2} \in \mathbb{C}$ . We can then follow the center manifold reduction in Theorem 4.1, but now we note that with high probability the quadratic self interaction term is non-zero. First, under the high probability scenarios outlined above, observe that

$$\begin{aligned} \sqrt{N} v_1 \circ v_1 &= a_2^2 \omega_{4k^*} + 2a_1 a_2 \omega_{3k^*} + a_1^2 \omega_{2k^*} + 2a_2 \bar{a}_1 \omega_{k^*} + (2a_1 \bar{a}_1 + 2a_2 \bar{a}_2) \omega_0 + 2a_1 \bar{a}_2 \omega_{-k^*} \\ &\quad + \bar{a}_1^2 \omega_{-2k^*} + 2\bar{a}_1 \bar{a}_2 \omega_{-3k^*} + \bar{a}_2^2 \omega_{-4k^*} + \mathcal{O}(\delta), \end{aligned} \quad (4.36)$$

giving that

$$\sqrt{N} \langle v_1, v_1 \circ v_1 \rangle = 3a_1^2 \bar{a}_2 + 3a_2 \bar{a}_1^2 + \mathcal{O}(\delta). \quad (4.37)$$

In this case the reduced flow on the center manifold is then described by the equation

$$\frac{dw_1}{dt} = \varepsilon w_1 + \frac{r\beta}{\sqrt{N}} w_1^2 + \mathcal{O}(3), \quad (4.38)$$

where  $\beta = 3a_1^2 \bar{a}_2 + 3a_2 \bar{a}_1^2 + \mathcal{O}(\delta)$ . If  $a_1 \neq 0$  and  $a_2 \neq 0$  then the quadratic coefficient is non-zero and  $\mathcal{O}(1)$  in  $\delta$ . The remainder of the proof is now straightforward and follows as in the previous result.  $\square$

## 5 Examples and Numerical Simulations

We conclude with a numerical investigation of (1.1) to illustrate our main results and to demonstrate how different the phenomena may be in the case where the hypothesis of our main result are not satisfied.

### 5.1 Example: small-world network

Consider the small-world graphon  $W(x, y)$ . Expanding the graphon as a Fourier Series

$$W(x, y) = \sum_{k \in \mathbb{Z}} c_k e^{2\pi i k(x-y)}, \quad (5.1)$$

we compute that

$$c_k = \left( \frac{p-q}{\pi k} \right) \sin(2\pi k \alpha), \quad c_0 = 2\alpha p + (1-2\alpha)q. \quad (5.2)$$

Hence, the graphon Laplacian eigenvalues are given by

$$\lambda_k = c_k - c_0 = \left( \frac{p-q}{\pi k} \right) \sin(2\pi k \alpha) - 2\alpha p - (1-2\alpha)q. \quad (5.3)$$

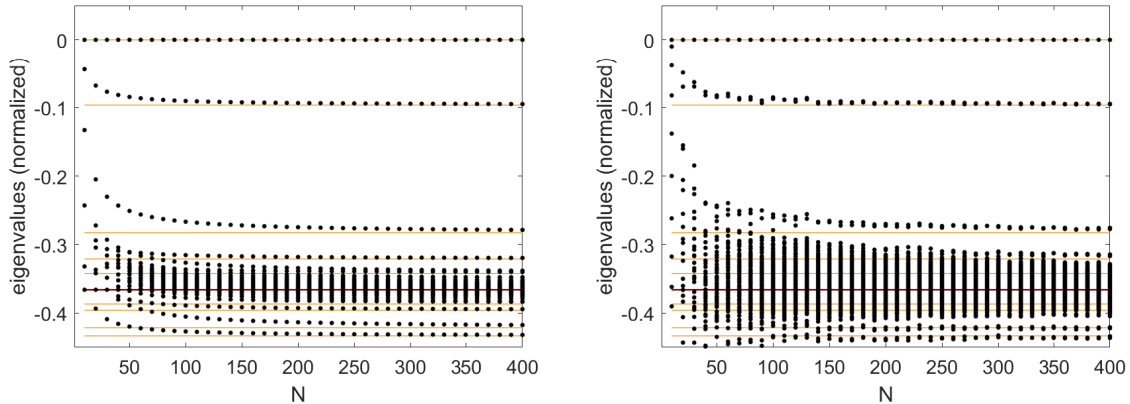


Figure 1: *Convergence of the (normalized) eigenvalues of the deterministic (left) and random (right) graph Laplacians for a small-world network with parameters  $(p, q, \alpha) = (0.90, 0.01, 0.20)$ . In both cases we show convergence of the eigenvalues for the graph Laplacians as the number of nodes is increased from  $N = 10$  to  $N = 400$ . In both figures the horizontal lines are the eigenvalues of the graphon defined in (5.3) for  $0 \leq k \leq 10$ . The darker line represents the accumulation point of the spectrum at  $\lambda_0 = c_0 = -0.366$ .*

In Figures 1-3 we present our numerical investigations of (1.1) for small-world graphs with parameters  $(p, q, \alpha) = (0.90, 0.01, 0.20)$  and system parameters  $(r, b) = (1, 1)$ . First, in Figure 1 we provide the eigenvalues of  $L_d$  and realizations of  $L_r$  for graphs of size  $N = 10$  to  $N = 400$ . Vertical lines represent the eigenvalues  $\lambda_k$  of the ring graphon Laplacian used to generate  $L_d$  and  $L_r$ . In both cases we see pairs of eigenvalues converging (after rescaling by  $N$ ) to the eigenvalues of the graphon Laplacian, confirming the analysis in Theorem 2.7. Note that the eigenvalue near  $-0.1$  of the graphon Laplacian is isolated and when  $N = 400$  the corresponding pair of eigenvalues of  $L_r$  are close to this isolated eigenvalue, meaning that Theorem 4.1 can be applied here. So, in Figure 2 we take a realization of the random graph with  $N = 400$  and numerically compute the pattern-forming Turing bifurcation curve in a neighborhood of  $(u, \varepsilon) = (0, 0)$  using numerical continuation. As predicted by our analysis, the bifurcation is weakly transcritical and resembles the supercritical pitchfork bifurcation predicted by the graphon analysis. We also plot the solution computed along this branch and observe that it closely resembles a translate of the bifurcating Fourier mode predicted by the graphon. To contrast this, we perform the same calculation for the fiftieth largest eigenvalue in Figure 3 using the same realization of the random graph. Here this eigenvalue is close to the accumulation point at  $c_0 = -0.3666$  (after normalizing by  $N = 400$ ) and is not sufficiently isolated to apply our analytical result. This is consistent with the numerical simulations, where the bifurcation is seen to be strongly transcritical and the bifurcating solution lacks any clear spatial structure.

## 5.2 Example: a graph with 2 : 1 resonance

To illustrate the results of Theorem 4.3, we consider the toy graphon model

$$W(x, y) = \frac{1}{2} + \frac{1}{4} \cos(2\pi(x - y)) + \frac{1}{4} \cos(4\pi(x - y)). \quad (5.4)$$

The above graphon has  $c_0 = \frac{1}{2}$ ,  $c_1 = c_2 = \frac{1}{8}$ , and all other  $c_k = 0$  in its Fourier expansion, and so the corresponding graphon Laplacian has eigenvalues given by  $0, -\frac{3}{8}, -\frac{1}{2}$ . Moreover, the eigenvalue  $-\frac{3}{8}$

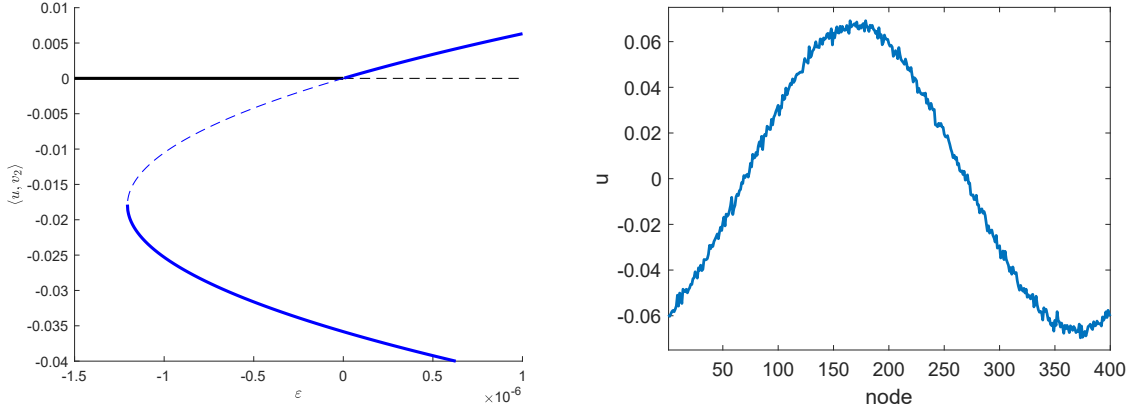


Figure 2: On the left is the bifurcation diagram near  $(u, \varepsilon) = (0, 0)$  for the discrete Swift–Hohenberg equation with  $(\kappa, r, b) = (-37.7255, 1, 1)$  on a random small-world network of size  $N = 400$  with parameters  $(p, q, \alpha) = (0.90, 0.01, 0.20)$ . Stable solutions are denoted by a solid line, while those that are unstable are given by a dashed line. Here  $\kappa$  corresponds to the largest (non-zero) eigenvalue of  $L_r$ . On the right is the bifurcating solution with  $\varepsilon = 0.0029$  which closely resembles a translate of the Fourier mode  $\cos(\frac{2\pi n}{400})$ . We note that the numerically computed quadratic interaction coefficient in this example is  $v^T v \circ v = 0.000515$ , where  $v$  is the eigenvector corresponding to the critical eigenvalue.

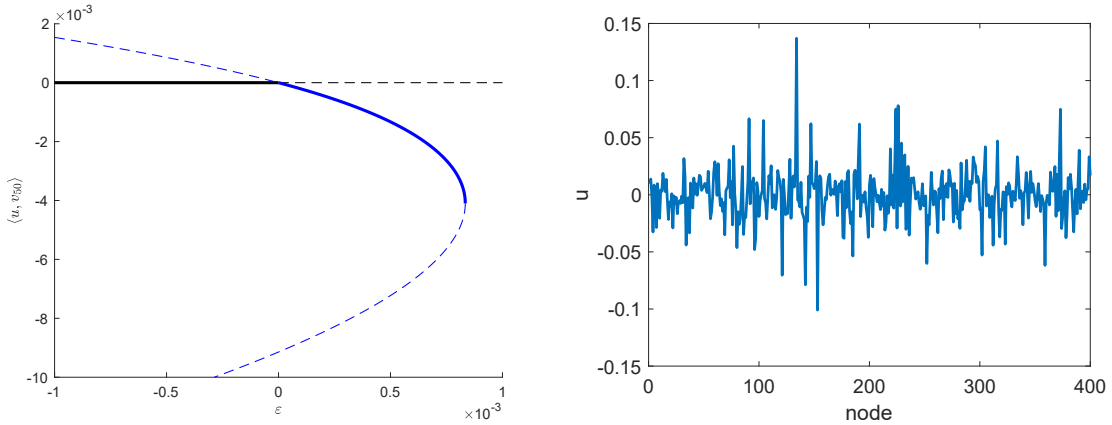


Figure 3: On the left is the bifurcation diagram near  $(u, \varepsilon) = (0, 0)$  for the discrete Swift–Hohenberg equation with  $(\kappa, r, b) = (-137.2908, 1, 1)$  on the same small-world network as in Figure 2. Here we take  $\kappa$  to be the fiftieth largest eigenvalue of  $L_r$ , which is not sufficiently isolated for the results of Section 4 to apply. Contrasting the axis scales in this figure with those of Figure 2, we see that the bifurcation is strongly transcritical in this case as compared to the example provided in Figure 2. The numerically computed quadratic interaction coefficient here is  $v^T v \circ v = -0.0157$ , where  $v$  is the eigenvector corresponding to the critical eigenvalue. This is a thirty fold increase over the coefficient obtained from the isolated principal eigenvalue. On the right we provide the bifurcating solution for  $\varepsilon = -0.0012$  where we observe a lack of spatial structure.

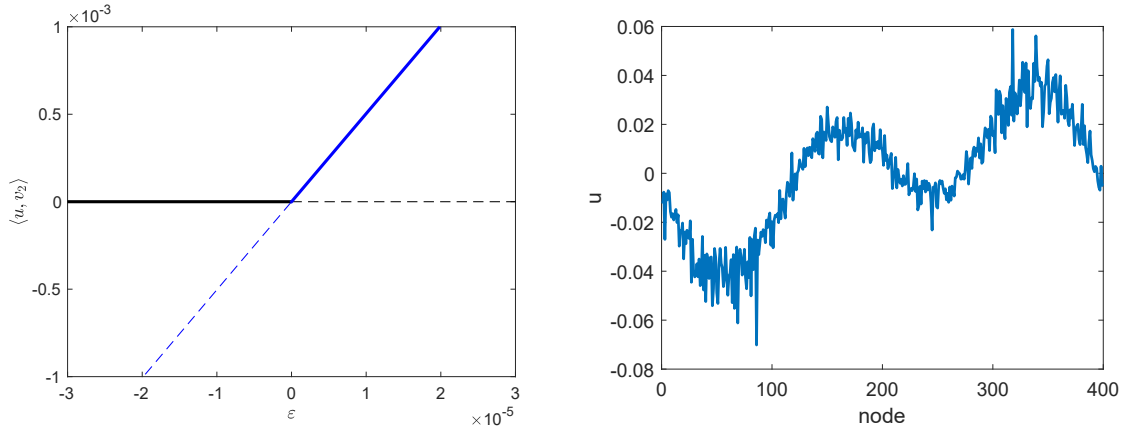


Figure 4: A transcritical bifurcation occurring due to the presence of a 2 : 1 resonance in the graphon (5.4). On the left is the bifurcation diagram near  $(u, \varepsilon) = (0, 0)$  for the discrete Swift–Hohenberg equation with  $(\kappa, r, b) = (-144.90, 1, 1)$ . On the right is the bifurcating solution for  $\varepsilon = -0.01$  where we notice that it resembles a superposition of the two bifurcating linear modes.

is isolated and comes in a 2 : 1 resonance since  $c_1 = c_2$ . For realizations of the random graph with  $N = 400$  nodes we find, as expected, that there are four eigenvalues near  $-\frac{3N}{8} = -150$ . The results of Theorem 4.3 shows that with high probability this configuration leads to a transcritical bifurcation. We further confirm these results with Figure 4, which shows a transcritical bifurcation with the bifurcating solution approximately a linear superposition of the involved Fourier modes.

### 5.3 Example: Bipartite graphs

For the final numerical exploration we turn to bipartite graphons. Recall from Section 2 that a bipartite graphon is given by

$$W(x, y) = \begin{cases} p & \min\{x, y\} \leq \alpha, \max\{x, y\} > \alpha \\ 0 & \text{otherwise} \end{cases} \quad (5.5)$$

with parameters  $p, \alpha \in (0, 1)$ . Recall further that if  $\alpha \neq \frac{1}{2}$ , then  $\text{Deg}(x)$ , the degree function defined in (2.12), is non-constant and therefore the results of Theorem 2.7 do not apply to the finite node graph Laplacians formed using the graphon  $W$ . Despite this analytical shortcoming, our numerical results indicate that Theorem 2.7 still applies to bipartite graphs, thus allowing one to study large bipartite graphs using bipartite graphons. Our goal is to illustrate this to the reader throughout this subsection. We begin with the following proposition that details the spectrum of bipartite graphon Laplacians.

**Proposition 5.1.** *Fix  $p, \alpha \in (0, 1)$  and let  $W$  be a bipartite graphon. Then, the bipartite graphon Laplacian satisfies  $\mathcal{L}_W f = \lambda f$  for some  $\lambda \in \mathbb{C}$  and  $f \in L^2$ , if and only if, one of the following is true:*

- (i)  $\lambda = 0$  and  $f$  is constant,
- (ii)  $\lambda = -p\alpha$ ,  $f(x) = 0$  for all  $x \in [0, \alpha)$ , and  $\int_\alpha^1 f(x)dx = 0$ ,
- (iii)  $\lambda = -p(1 - \alpha)$ ,  $f(x) = 0$  for all  $x \in (\alpha, 1]$ , and  $\int_0^\alpha f(x)dx = 0$ ,

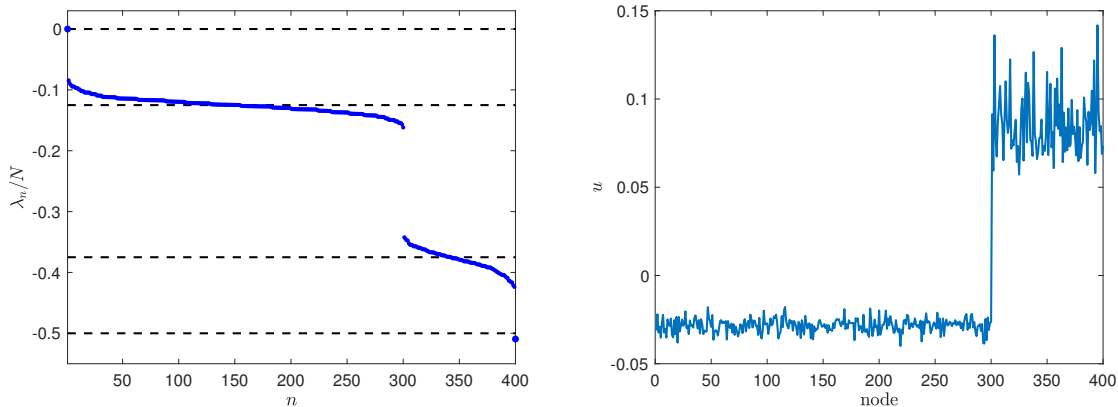


Figure 5: On the left are the eigenvalues,  $\lambda_n$  (blue dots), of a random bipartite graph with  $N = 400$  nodes and parameter values  $(p, \alpha) = (0.5, 0.75)$ . Eigenvalues are normalized by the number of nodes so they can be seen to be clustering about the values of eigenvalues of the bipartite graphon Laplacian (dashed horizontal lines) from Proposition 5.1. On the right is the eigenfunction associated to  $\lambda_{400}$ , the isolated eigenvalue near  $-pN$ , which is approximately given by a piecewise constant function, closely resembling the eigenfunction of the bipartite graphon Laplacian that spans the  $\lambda = -p$  eigenspace.

(iv)  $\lambda = -p$ , there exists a constant  $C \in \mathbb{R}$  such that  $f(x) = (1 - \alpha)C$  for all  $x \in [0, \alpha)$ , and  $f(x) = -\alpha C$  for all  $x \in (\alpha, 1]$ .

*Proof.* With  $W(x, y)$  as given in (5.5), one finds that

$$[\mathcal{L}_W f](x) = \begin{cases} p \int_{\alpha}^1 f(y) dy - f(x)p(1 - \alpha), & x \leq \alpha, \\ p \int_0^{\alpha} f(y) dy - f(x)p\alpha, & x > \alpha, \end{cases} \quad (5.6)$$

for all  $x \in [0, 1]$ . The result then follows by setting  $\mathcal{L}f = \lambda f$  and working through the distinct cases.  $\square$

From Proposition 5.1 we see that there are only four possible choices for eigenvalues of the bipartite graphon Laplacian. Moreover, eigenvalues  $\lambda = 0, -p$  are isolated with one-dimensional eigenspaces, while the eigenvalues  $\lambda = -p\alpha, -p(1 - \alpha)$  have infinite-dimensional eigenspaces. This can be observed from the fact that the eigenfunctions can be obtained from any mean-zero function on either  $[0, \alpha]$  or  $[\alpha, 1]$ . Such functions can be represented uniquely as Fourier series with zero constant term, meaning that the trigonometric terms that make up the series can be used to span the entire eigenspace. Most important to our work here is that numerically we observe that the random graph Laplacians generated using bipartite graphons have eigenvalues that cluster around the four eigenvalues of the bipartite graphon Laplacian. We illustrate this in Figure 5 where we present the eigenvalues of a random bipartite graph Laplacian with  $N = 400$  nodes and parameter values  $(p, \alpha) = (0.5, 0.75)$ . Upon normalizing by the size of the graph, one can see the clustering of the random graph eigenvalues near the eigenvalues of the graphon Laplacian. We also provide the eigenfunction of the smallest eigenvalue,  $\lambda_{400} \approx -pN = -200$ , which resembles a step function that is constant on  $[0, \alpha)$  and  $(\alpha, 1]$ , similar to the eigenfunction that spans the one-dimensional eigenspace of  $\lambda = -p$  for the graphon Laplacian. We have documented nearly identical results for other choices of the parameters  $p$  and  $\alpha$ .

With the isolated eigenvalues  $\lambda = 0, -p$  of the bipartite graphon Laplacian, one may follow the analysis of Sections 3 and 4 to identify the pattern forming bifurcations for both the continuous-space graphons and the discrete-space random graphs. Interestingly, one finds that the graphon bifurcations are transcritical, as opposed to the pitchfork bifurcations in the ring network case. Since transcritical bifurcations are robust with respect to perturbations, one similarly expects large random bipartite graphs to experience transcritical pattern-forming bifurcations from the eigenvalues near 0 and  $-pN$ , where  $N$  is the number of nodes in the network. Although not provided here for brevity, our numerical results have confirmed this by observing transcritical bifurcations from these eigenvalues on large random bipartite graphs for a range of parameters  $p$  and  $\alpha$ .

Finally, we similarly expect that multipartite graphons can be used to study steady-state bifurcations from isolated eigenvalues of large random multipartite graphs with equally as promising results to those that we have provided for ring networks in the preceding sections. We conjecture that our results in Theorem 2.7 hold for multipartite graphons as well, since the only major distinction in the analysis is that multipartite graphons have  $\text{Deg}(x)$  being a piecewise constant function, as opposed to the ring network case where they are constant.

## 6 Discussion

In this work we have shown how graphons can be used to study pattern-forming Turing bifurcations in spatially-discrete Swift–Hohenberg equations on large random graphs. In particular, the work in Section 2 provides the necessary functional analytical theory to detail how isolated elements of the graphon’s spectrum can be used to approximate eigenvalues and eigenvectors of both deterministic and random graphs formed from the graphon. Importantly, the study of graphons allows one to quantify the spectrum of classes of large random graphs, thus providing a novel avenue to study pattern formation on networks which goes far beyond working with regular and idealized graph structures, such as chains and rings. In Section 3 we described Turing bifurcations from the trivial state  $u = 0$  in the infinite-dimensional graphon Swift–Hohenberg equation. In Section 4 we then leveraged the results of Section 2 to compare the graphon bifurcations with the Turing bifurcations in the Swift–Hohenberg equation posed on large random graphs. We found that the pitchfork bifurcations observed in the graphon setting degenerates into a transcritical bifurcation with a saddle-node nearby when space is discretized to obtain the finite-dimensional graphs.

Our numerical results in Section 5 provide positive affirmation of our theoretical work in the preceding sections. That is, we were able to observe the degeneration from pitchfork to transcritical bifurcations coming from isolated, non-resonant eigenvalues in the spectrum of small-world random graphs. We also provided an example of a graphon which has resonant eigenvalues, thus necessitating Theorem 4.3 to describe these Turing bifurcations, again leading to a confirmation of our theoretical results. Our final numerical consideration was that of bipartite graphons, which are not covered by the work in this manuscript. Nonetheless, we found that again the spectrum of the large random bipartite graphs asymptotically cluster about the spectrum of bipartite graphons, as was shown in Figure 5. This indicates that our results are applicable to a wider class of graphons than the ring networks that we restricted ourselves to throughout this work. Hence, in future investigations it will be important to determine the widest possible class of graphons for which our results can apply. Conversely, it is necessary to identify graphons for which our theoretical results herein differ so that follow-up studies can identify their expected pattern-forming bifurcations as

well.

It is important to emphasize that our construction of deterministic and random graphs from graphons results in dense networks. That is, the degree of each vertex positively scales with the number of vertices in the graph. Related work motivated by the study of coupled oscillators into semilinear heat equations has extended results from dense graphs to sparse graphs, meaning that the edge density goes to zero as the number of vertices goes to infinity [21]. Therefore, it is our intention to extend the work in this manuscript to the study of pattern-formation on sparse random graphs, potentially by taking advantage of the recent developments in [4] which details how to use graphons to construct sequences of sparse graphs.

Finally, we comment on localized patterns on the graph that may be a consequence of the Turing bifurcations detailed in this manuscript. Note that the degeneration of the pitchfork bifurcations from graphon networks to graph networks typically leads to regions of bistability in the spatially-discrete Swift–Hohenberg equation. This can be observed, for example, in Figure 2 for the small-world network. The competition between states in regions of bistability has been shown to result in steady-state localized patterns for which a connected subset of the elements are near the stable patterned state, while the remaining elements on the graph are near the homogeneous state  $u = 0$  [6, 7, 40]. It remains to identify if such localized states exist in the small regions of bistability observed in the random graph networks studied here. Since the networks are dense, one expects that the bifurcation curves of localized solutions (if they exist) strongly resemble the simple closed curves of localized patterns on ring networks with all-to-all coupling detailed in [40]. Initial numerical investigations have been unsuccessful in identifying such localized patterns, but without analytical proofs that such steady-state solutions exist or not these investigations are inconclusive. Therefore, we leave the study of localized steady-states on random graphs to a follow-up investigation.

## Acknowledgments

The research of MH was partially supported by the National Science Foundation through NSF-DMS-2007759. MH is grateful Ben Concepcion for contributing to a preliminary iteration of this project.

## References

- [1] S.-I. Amari. Dynamics of pattern formation in lateral-inhibition type neural fields. *Biological cybernetics*, 27(2):77–87, 1977.
- [2] C. Borgs, J. Chayes, L. Lovász, V. Sós, and K. Vesztegombi. Limits of randomly grown graph sequences. *European Journal of Combinatorics*, 32(7):985–999, 2011.
- [3] C. Borgs, J. T. Chayes, H. Cohn, and N. Holden. Sparse exchangeable graphs and their limits via graphon processes. *arXiv preprint arXiv:1601.07134*, 2016.
- [4] C. Borgs, J. T. Chayes, H. Cohn, and Y. Zhao. An  $L^p$  theory of sparse graph convergence I: Limits, sparse random graph models, and power law distributions. *Trans. Amer. Math. Soc.*, 372(5):3019–3062, 2019.
- [5] J. J. Bramburger. Isolates of multi-pulse solutions to lattice dynamical systems. *Proceedings of the Royal Society of Edinburgh Section A: Mathematics*, 151(3):916–952, 2021.

- [6] J. J. Bramburger and B. Sandstede. Spatially localized structures in lattice dynamical systems. *Journal of Nonlinear Science*, pages 1–42, 2019.
- [7] J. J. Bramburger and B. Sandstede. Localized patterns in planar bistable weakly coupled lattice systems. *Nonlinearity*, 33(7):3500, 2020.
- [8] P. C. Bressloff. New mechanism for neural pattern formation. *Physical Review Letters*, 76(24):4644, 1996.
- [9] V. Castets, E. Dulos, J. Boissonade, and P. De Kepper. Experimental evidence of a sustained standing turing-type nonequilibrium chemical pattern. *Physical review letters*, 64(24):2953, 1990.
- [10] H. Chiba and G. S. Medvedev. The mean field analysis of the Kuramoto model on graphs II. Asymptotic stability of the incoherent state, center manifold reduction, and bifurcations. *Discrete Contin. Dyn. Syst.*, 39(7):3897–3921, 2019.
- [11] H. Chiba, G. S. Medvedev, and M. S. Mizuhara. Bifurcations in the Kuramoto model on graphs. *Chaos*, 28(7):073109, 10, 2018.
- [12] M. C. Cross and P. C. Hohenberg. Pattern formation outside of equilibrium. *Rev. Mod. Phys.*, 65:851–1112, Jul 1993.
- [13] C. Davis and W. M. Kahan. The rotation of eigenvectors by a perturbation. iii. *SIAM Journal on Numerical Analysis*, 7(1):1–46, 1970.
- [14] G. B. Ermentrout and J. D. Cowan. A mathematical theory of visual hallucination patterns. *Biological cybernetics*, 34(3):137–150, 1979.
- [15] A. Gierer and H. Meinhardt. A theory of biological pattern formation. *Kybernetik*, 12(1):30–39, 1972.
- [16] D. Glasscock. What is... a graphon. *Notices of the AMS*, 62(1), 2015.
- [17] M. Haragus and G. Iooss. *Local bifurcations, center manifolds, and normal forms in infinite-dimensional dynamical systems*. Universitext. Springer-Verlag London, Ltd., London; EDP Sciences, Les Ulis, 2011.
- [18] J. J. Hopfield. Neurons with graded response have collective computational properties like those of two-state neurons. *Proceedings of the National Academy of Sciences*, 81(10):3088–3092, 1984.
- [19] Y. Ide, H. Izuhara, and T. Machida. Turing instability in reaction-diffusion models on complex networks. *Physica A: Statistical Mechanics and its Applications*, 457:331–347, 2016.
- [20] S. Janson. *Graphons, cut norm and distance, couplings and rearrangements*, volume 4 of *New York Journal of Mathematics. NYJM Monographs*. State University of New York, University at Albany, Albany, NY, 2013.
- [21] D. Kaliuzhnyi-Verbovetskyi and G. S. Medvedev. The semilinear heat equation on sparse random graphs. *SIAM J. Math. Anal.*, 49(2):1333–1355, 2017.
- [22] E. F. Keller and L. A. Segel. Initiation of slime mold aggregation viewed as an instability. *Journal of theoretical biology*, 26(3):399–415, 1970.



- [23] C. A. Klausmeier. Regular and irregular patterns in semiarid vegetation. *Science*, 284(5421):1826–1828, 1999.
- [24] S. Kondo. An updated kernel-based Turing model for studying the mechanisms of biological pattern formation. *J. Theoret. Biol.*, 414:120–127, 2017.
- [25] S. Kondo and T. Miura. Reaction-diffusion model as a framework for understanding biological pattern formation. *Science*, 329(5999):1616–1620, 2010.
- [26] C. Kuehn and S. Thom. Power network dynamics on graphons. *SIAM J. Appl. Math.*, 79(4):1271–1292, 2019.
- [27] L. Lovász. *Large networks and graph limits*, volume 60 of *American Mathematical Society Colloquium Publications*. American Mathematical Society, Providence, RI, 2012.
- [28] L. Lovász and B. Szegedy. Limits of dense graph sequences. *J. Combin. Theory Ser. B*, 96(6):933–957, 2006.
- [29] N. McCullen and T. Wagenknecht. Pattern formation on networks: From localised activity to turing patterns. *Scientific reports*, 6(1):1–8, 2016.
- [30] G. S. Medvedev. The nonlinear heat equation on dense graphs and graph limits. *SIAM J. Math. Anal.*, 46(4):2743–2766, 2014.
- [31] G. S. Medvedev. The nonlinear heat equation on  $W$ -random graphs. *Arch. Ration. Mech. Anal.*, 212(3):781–803, 2014.
- [32] M. Mimura and J. Murray. On a diffusive prey-predator model which exhibits patchiness. *Journal of Theoretical Biology*, 75(3):249–262, 1978.
- [33] P. K. Moore and W. Horsthemke. Localized patterns in homogeneous networks of diffusively coupled reactors. *Physica D: Nonlinear Phenomena*, 206(1):121–144, 2005.
- [34] R. Muolo, M. Asllani, D. Fanelli, P. K. Maini, and T. Carletti. Patterns of non-normality in networked systems. *Journal of Theoretical Biology*, 480:81–91, 2019.
- [35] H. Nakao and A. S. Mikhailov. Turing patterns in network-organized activator–inhibitor systems. *Nature Physics*, 6(7):544–550, 2010.
- [36] A. C. Newell and J. A. Whitehead. Finite bandwidth, finite amplitude convection. *Journal of Fluid Mechanics*, 38(2):279–303, 1969.
- [37] R. I. Oliveira. Concentration of the adjacency matrix and of the laplacian in random graphs with independent edges. *arXiv preprint arXiv:0911.0600*, 2009.
- [38] H. Othmer and L. Scriven. Instability and dynamic pattern in cellular networks. *Journal of Theoretical Biology*, 32(3):507–537, 1971.
- [39] Q. Ouyang and H. L. Swinney. Transition from a uniform state to hexagonal and striped turing patterns. *Nature*, 352(6336):610–612, 1991.

- [40] M. Tian, J. J. Bramburger, and B. Sandstede. Snaking bifurcations of localized patterns on ring lattices. *IMA Journal of Applied Mathematics*, 06 2021.
- [41] A. M. Turing. The chemical basis of morphogenesis. *Philosophical Transactions of the Royal Society of London Series B*, 237(641):37–72, 1952.
- [42] A. Volkening and B. Sandstede. Iridophores as a source of robustness in zebrafish stripes and variability in danio patterns. *Nature communications*, 9(1):1–14, 2018.
- [43] M. Wolfrum. The Turing bifurcation in network systems: Collective patterns and single differentiated nodes. *Physica D: Nonlinear Phenomena*, 241(16):1351–1357, 2012.
- [44] Y. Yu, T. Wang, and R. J. Samworth. A useful variant of the Davis–Kahan theorem for statisticians. *Biometrika*, 102(2):315–323, 2015.